renin activity and aldosterone concentration were determined by radioimmunoassays as previously reported [11], and serum insulin level was measured by an enzyme immunoassay. Serum lipid and glucose levels were measured with an automatic analyzer (OLYMPUS AU2700, OLYMPUS, Tokyo, Japan), and serum creatinine levels were determined by an enzymatic method.

2.3. Statistical analysis

All the data were analyzed with SPSS software version 17.0 (SPSS Inc., Chicago, IL, USA). Comparisons between two groups were assessed by the unpaired *t*-test or chi-squared test, and correlations between two parameters were tested by simple regression analysis. The relationships were further analyzed by multiple regression analysis with a step-wise method to identify the factor(s) independently associated with the plasma levels of AM–NH_2 and AM–Gly. In this multivariate analysis, the basal or metabolic factors that were found to be significant by simple regression were used as independent covariates. All the data are expressed as means ± S.D., and *P* values of less than 0.05 were considered to be significant.

3. Results

In a comparison of the basal clinical data from the non-obese and obese residents (Table 1), no significant differences were noted in gender, age, or serum creatinine levels, while both the systolic and diastolic blood pressure (SBP and DBP) levels of the obese subjects were higher than those of the non-obese subjects. The results of the measurement of metabolic and humoral factors are shown in Table 2, where obesity-related metabolic parameters such as the blood levels of fasting glucose, insulin, high-density lipoprotein-cholesterol (HDL-cholesterol), triglycerides, and the homeostasis model assessment (HOMA) index of the subjects with obesity are shown to be higher than those without obesity, but this was not the case for serum total cholesterol level, plasma renin activity, or aldosterone concentration.

As shown in Fig. 1, the plasma levels of total AM, AM–NH_2, and AM–Gly were all significantly elevated in the obese subjects compared with the non-obese subjects. Table 3 shows the coefficients of correlation obtained by simple regression analyses of the relationships between two AM values and other basal, metabolic, or humoral parameters in the subjects. Both the AM–NH_2 and AM–Gly level were significantly correlated with BMI, SBP, and DBP, and significant relationships were observed between the AM–NH_2 level and age and between the AM–Gly and serum creatinine levels. In the analyses of the metabolic and humoral data, we found that the AM–NH_2 level was significantly correlated with serum triglyceride levels, while the AM–Gly level was correlated with all the parameters listed in Table 3. These significant relationships between the two AM values and BMI or metabolic or humoral factors are shown in Figs. 2 and 3 by scattered plotting.

We further analyzed the relationships by means of multivariate analysis with a step-wise method in order to identify the independently significant factors for the two AM values. As shown in Table 4, BMI and the serum triglyceride levels were found to be independently significant for the AM–NH_2 level, while DBP, insulin and HDL-cholesterol levels, and plasma renin activity were significant for the AM–Gly level. To look at gender differences in plasma AM levels, we also carried out multivariate analysis including gender in addition to the significant parameters presented in Table 3, but gender was not extracted as a significant factor of the plasma levels of AM–NH_2 or AM–Gly.

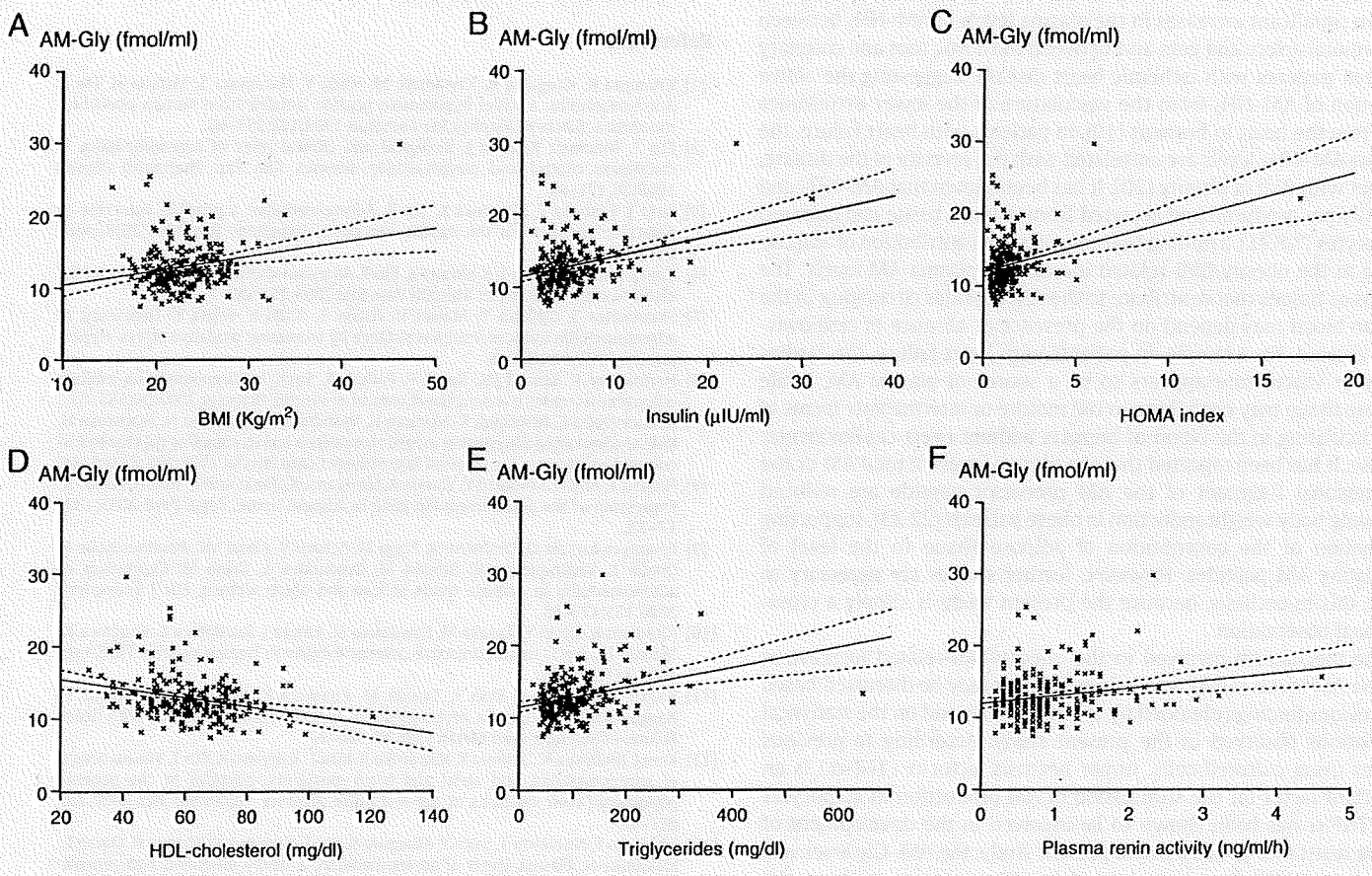

Fig. 3. Relationships between the AM–Gly and BMI (A), insulin (B), HOMA index (C), HDL-cholesterol (D), triglyceride (E) levels, or plasma renin activity (F). Regression lines and 95% confidence limits are shown on each graph.

Table 4
Multiple regression analysis with a step-wise method.

Dependent variables	Independent covariates	β	P
AM-NH_2	BMI	.185	.006
	Triglycerides	.154	.022
AM-Gly	DBP	.210	.001
	Insulin	.177	.008
	HDL-cholesterol	−.178	.006
	Plasma renin activity	.177	.005

The independent covariates included in this analysis were those judged to be significant by the simple regression analysis (Table 3).
The abbreviations are listed in Tables 1 and 2.

4. Discussion

Two molecular forms of AM circulate in the blood of humans and rats; one is a mature form of AM with an amidated C-terminal (AM-NH_2), and the other is an intermediate form with a non-amidated C-terminal glycine (AM-Gly) [14,18]. There are a number of reports on AM measurements in plasma and tissue, but in most of these cases, the immunoreactive AM detected was the total AM level consisting of both AM-NH_2 and AM-Gly [2–4,14]. Using a radioimmunoassay to detect total AM levels, we have previously reported a significant relationship between plasma AM levels and BMI in subjects who had undergone a regular medical check-up [12], and an obesity-related increase in the plasma AM level has also been reported in an animal model of obesity [8]. In the present study, we measured the plasma levels of AM with two types of immunoreactive radiometric assays that detect total and mature AM, respectively, and found that both the AM-NH_2 and AM-Gly levels were elevated in subjects with obesity according to their BMI, as compared to those who were not obese.

Cultured cells isolated from the blood vessels or myocardium have been shown to produce and secrete AM [3,4]. We have previously shown significant increases in the plasma levels of AM-NH_2 between the femoral artery and vein and between the aortic root and coronary sinus in patients with ischemic heart disease, suggesting the active secretion of AM-NH_2 from the vasculature of the lower extremities and from the heart in humans [19]. In patients with heart failure, the plasma AM-NH_2 levels are correlated with the severity of the disease, but not with BMI or obesity [20]. It has been shown that AM-NH_2 and AM-Gly are produced and secreted from adipose tissue and cultured adipocytes [7,8,21], a finding that suggests the contribution of adipose tissue to the obesity/BMI-related increase in plasma AM levels. The organs or tissues that contribute to the AM peptides circulating in the human blood may depend on the presence or absence of cardiovascular disease. For example, in patients with heart failure, the cardiac tissue or vasculature appears to be a source of plasma AM, while adipose tissue may contribute to the mature or intermediate forms of AM circulating in the blood of humans without overt cardiovascular disease. It has been reported that the plasma levels of total AM or the mid-regional fragment of the AM precursor peptide are reduced following body weight reduction in obese patients [22,23], supporting the notion of the contribution of adipose tissue to the level of circulating AM peptides. However, further studies are necessary to prove this hypothesis, because the present study is simply a cross-sectional observation.

The mechanism involved in the obesity/BMI-related increase in plasma AM levels remains to be clarified but may be discussed based on previous findings obtained by in vitro studies and on the statistical correlations observed in the present study. According to previous studies using cultured cells, tumor necrosis factor-α (TNF-α) is an important factor for the stimulation of AM production in adipocytes [21]. TNF-α has been shown to be involved in the development of insulin resistance [24,25]. In the present study, the AM-Gly level was related to metabolic parameters of insulin resistance such as the HOMA index, HDL-cholesterol, and triglycerides, suggesting a role for TNF-α in the BMI/obesity-related increase. We may also need to note the significant correlation between the AM-Gly level and plasma renin activity, because the renin–angiotensin system has been shown to be an important factor for stimulating AM production and secretion [2–4]. In the present study, the findings of interest include the differences in the correlation coefficients obtained by simple regression and in the significant factors demonstrated by the multivariate analysis between AM-NH_2 and AM-Gly. According to our previous studies [14,26,27], it is possible that the AM-NH_2 levels in plasma depend on at least two factors: enzymatic amidation activity and peptide clearance by receptor binding. These factors may have been involved in producing the different results of the simple and multiple regression analyses between AM-NH_2 and AM-Gly.

Lastly, we need to discuss the role(s) of AM-NH_2 and AM-Gly in plasma, the levels of which were elevated in relation to increased BMI and/or obesity. AM has been shown to have a wide range of actions including blood pressure reduction, modulation of adipogenesis, and alleviation of insulin resistance [2–7]. AM-Gly itself is biologically inactive, but we showed that AM-Gly exerts vasodilatory action following conversion into AM-NH_2 in isolated rat aortas ex vivo [27]. In this experiment, AM-Gly took a much longer time to reach the maximal relaxation than did AM-NH_2, suggesting a role for AM-Gly as a hormone reservoir. Based on the correlations between the two molecular forms of AM and the other clinical parameters, we speculate that AM acts against the development of a number of obesity-induced disorders such as insulin resistance and elevated blood pressure.

In conclusion, the present study showed that both the AM-NH_2 and AM-Gly levels in plasma are elevated in subjects with increased BMI or obesity without overt cardiovascular disease. The correlations between the plasma AM levels and the other clinical parameters suggest a possible, active role for this bioactive peptide in metabolic disorders associated with obesity.

References

[1] Kitamura K, Kangawa K, Kawamoto M, Ichiki Y, Nakamura S, Matsuo H, Eto T. Adrenomedullin: a novel hypotensive peptide isolated from human pheochromocytoma. Biochem Biophys Res Commun 1993;192:553–60.
[2] Eto T, Kitamura K, Kato J. Biological and clinical roles of adrenomedullin in circulation control and cardiovascular diseases. Clin Exp Pharmacol Physiol 1999;26:371–80.
[3] Kato J, Tsuruda T, Kitamura K, Eto T. Adrenomedullin: a possible autocrine or paracrine hormone in the cardiac ventricles. Hypertens Res 2003;26(Suppl): S113–9.
[4] Kato J, Tsuruda T, Kita T, Kitamura K, Eto T. Adrenomedullin: a protective factor for blood vessels. Arterioscler Thromb Vasc Biol 2005;25:2480–7.
[5] Shimosawa T, Ogihara T, Matsui H, Asano T, Ando K, Fujita T. Deficiency of adrenomedullin induces insulin resistance by increasing oxidative stress. Hypertension 2003;41:1080–5.
[6] Harmancey R, Senard JM, Rouet P, Pathak A, Smih F. Adrenomedullin inhibits adipogenesis under transcriptional control of insulin. Diabetes 2007;56:553–63.
[7] Iemura-Inaba C, Nishikimi T, Akimoto K, Yoshihara F, Minamino N, Matsuoka H. Role of adrenomedullin system in lipid metabolism and its signaling mechanism in cultured adipocytes. Am J Physiol Regul Integr Comp Physiol 2008;295:R1376–84.
[8] Nambu T, Arai H, Komatsu Y, Yasoda A, Moriyama K, Kanamoto N, Itoh H, Nakao K. Expression of the adrenomedullin gene in adipose tissue. Regul Pept 2005;132: 17–22.
[9] Paulmyer-Lacroix O, Desbriere R, Poggi M, Achard V, Alessi MC, Boudouresque F, Ouafik L, Vuaroqueaux V, Labuhn M, Dutourand A, Grino M. Expression of adrenomedullin in adipose tissue of lean and obese women. Eur J Endocrinol 2006;155:177–85.
[10] Kitamura K, Ichiki Y, Tanaka M, Kawamoto M, Emura J, Sakakibara S, Kangawa K, Matsuo H, Eto T. Immunoreactive adrenomedullin in human plasma. FEBS Lett 1994;341:288–90.
[11] Kato J, Kobayashi K, Etoh T, Tanaka M, Kitamura K, Imamura T, Koiwaya Y, Kangawa K, Eto T. Plasma adrenomedullin concentration in patients with heart failure. J Clin Endocrinol Metab 1996;81:180–3.
[12] Kato J, Kitamura K, Uemura T, Kuwasako K, Kita T, Kangawa K, Eto T. Plasma levels of adrenomedullin and atrial and brain natriuretic peptides in the general population: their relations to age and pulse pressure. Hypertens Res 2002;25: 887–92.
[13] Ishimitsu T, Nishikimi T, Saito Y, Kitamura K, Eto T, Kangawa K, Matsuo H, Omae T, Matsuoka H. Plasma levels of adrenomedullin, a newly identified hypotensive peptide, in patients with hypertension and renal failure. J Clin Invest 1994;94: 2158–61.

[14] Kitamura K, Kato J, Kawamoto M, Tanaka M, Chino N, Kangawa K, Eto T. The intermediate form of glycine-extended adrenomedullin is the major circulating molecular form in human plasma. Biochem Biophys Res Commun 1998;244: 551–5.
[15] Examination Committee of Criteria for 'Obesity Disease' in Japan. Japan Society for the Study of Obesity: new criteria for 'obesity disease' in Japan. Circ J 2002;66: 987–92.
[16] Ohta H, Tsuji T, Asai S, Sasakura K, Teraoka H, Kitamura K, Kangawa K. One-step direct assay for mature-type adrenomedullin with monoclonal antibodies. Clin Chem 1999;45:244–51.
[17] Ohta H, Tsuji T, Asai S, Tanizaki S, Sasakura K, Teraoka H, Kitamura K, Kangawa K. A simple immunoradiometric assay for measuring the entire molecules of adrenomedullin in human plasma. Clin Chim Acta 1999;287:131–43.
[18] Yamaga J, Hashida S, Kitamura K, Tokashiki M, Aoki T, Inatsu H, Ishikawa N, Kangawa K, Morishita K, Eto T. Direct measurement of glycine-extended adrenomedullin in plasma and tissue using an ultrasensitive immune complex transfer enzyme immunoassay in rats. Hypertens Res 2003;26(Suppl):S45–53.
[19] Hirayama N, Kitamura K, Imamura T, Kato J, Koiwaya Y, Eto T. Secretion and clearance of the mature form of adrenomedullin in humans. Life Sci 1999;64: 2505–9.
[20] Hirayama N, Kitamura K, Imamura T, Kato J, Koiwaya Y, Tsuji T, Kangawa K, Eto T. Molecular forms of circulating adrenomedullin in patients with congestive heart failure. J Endocrinol 1999;160:297–303.
[21] Li Y, Totsune K, Takeda K, Furuyama K, Shibahara S, Takahashi K. Differential expression of adrenomedullin and resistin in 3T3-L1 adipocytes treated with tumor necrosis factor-alpha. Eur J Endocrinol 2003;149:231–8.
[22] Minami J, Nishikimi T, Ishimitsu T, Makino Y, Kawano Y, Takishita S, Kangawa K, Matsuoka H. Effect of a hypocaloric diet on adrenomedullin and natriuretic peptides in obese patients with essential hypertension. J Cardiovasc Pharmacol 2000;36(Suppl 2):S83–6.
[23] Vila G, Riedl M, Maier C, Struck J, Morgenthaler NG, Handisurya A, Prager G, Ludvik B, Clodi M, Luger A. Plasma MR-proADM correlates to BMI and decreases in relation to leptin after gastric bypass surgery. Obesity 2009;17:1184–8.
[24] Hotamisligil GS, Peraldi P, Budavari A, Ellis R, White MF, Spiegelman BM. IRS-1-mediated inhibition of insulin receptor tyrosine kinase activity in TNF-alpha- and obesity-induced insulin resistance. Science 1996;271:665–8.
[25] Uysal KT, Wiesbrock SM, Marino MW, Hotamisligil GS. Protection from obesity-induced insulin resistance in mice lacking TNF-alpha function. Nature 1997;389: 610–4.
[26] Ishiyama Y, Kitamura K, Ichiki Y, Sakata J, Kida O, Kangawa K, Eto T. Haemodynamic responses to rat adrenomedullin in anaesthetized spontaneously hypertensive rats. Clin Exp Pharmacol Physiol 1995;22:614–8.
[27] Cao YN, Kitamura K, Ito K, Kato J, Hashida S, Morishita K, Eto T. Glycine-extended adrenomedullin exerts vasodilator effect through amidation in the rat aorta. Regul Pept 2003;113:109–14.

Cephalalgia
An International Journal of Headache
International Headache Society

doi:10.1111/j.1468-2982.2008.01695.x

Effect of adrenomedullin on the cerebral circulation: relevance to primary headache disorders

KA Petersen[1,2], S Birk[1,2], K Kitamura[3] & J Olesen[1,2]

[1]Danish Headache Centre, University of Copenhagen, Copenhagen and [2]Department of Neurology, Glostrup University Hospital, Glostrup, Denmark, and [3]First Department of Internal Medicine, Miyazaki Medical College, University of Miyazaki, Miyazaki, Japan

Cephalalgia

Petersen KA, Birk S, Kitamura K & Olesen J. Effect of adrenomedullin on the cerebral circulation: relevance to primary headache disorders. Cephalalgia 2009; 29:23–30. London. ISSN 0333-1024

Adrenomedullin (ADM) is closely related to calcitonin gene-related peptide, which has a known causative role in migraine. Animal studies have strongly suggested that ADM has a vasodilatory effect within the cerebral circulation. For these reasons, ADM is also likely to be involved in migraine. However, the hypothetical migraine-inducing property and effect on human cerebral circulation of ADM have not previously been investigated. Human ADM (0.08 g kg^{-1} min^{-1}) or placebo (saline 0.9%) was administered as a 20-min intravenous infusion to 12 patients suffering from migraine without aura in a crossover double-blind study. The occurrence of headache and associated symptoms were registered regularly 24 h post infusion. Cerebral blood flow (CBF) was measured by ^{133}Xenon single-photon emission computed tomography, mean blood flow velocity in the middle cerebral artery (V_{MCA}) by transcranial Doppler and the diameter of peripheral arteries by transdermal ultrasound (C-scan). ADM did not induce significantly more headache or migraine compared with placebo ($P = 0.58$). CBF was unaffected by ADM infusion (global CBF, $P = 0.32$ and $rCBF_{MCA}$, $P = 0.38$) and the same applied for the V_{MCA} ($P = 0.18$). The superficial temporal artery dilated compared with placebo ($P < 0.001$), and facial flushing was seen after ADM administration ($P = 0.001$). In conclusion, intravenous ADM is not a mediator of migraine headache and does not dilate intracranial arteries. □*Adrenomedullin, cerebral blood flow, vasodilatation, migraine*

Kenneth A. Petersen, MD, PhD, Danish Headache Centre, University Hospital of Copenhagen and Department of Neurology, Glostrup University Hospital, DK-2600 Glostrup, Denmark. Tel. + 45 3810-0448, e-mail kapetersen@dadlnet.dk *Received 16 August 2007, accepted 1 May 2008*

Introduction

There is strong evidence of a pivotal role of calcitonin gene-related peptide (CGRP) and nitric oxide (NO) in migraine pathogenesis (1–6). However, other substances may be involved, and a member of the CGRP family, adrenomedullin (ADM), is an obvious candidate for further investigation.

ADM was discovered 10 years ago among peptides extracted from pheochromocytomas (7). Subsequently, its pharmacological and physiological properties have been defined (8). The mRNA of the peptide, originating from a single locus on chromosome 11 (9), is found in the highest concentration in endothelial cells (10) and in particular within the cerebral circulation (11). From the precursor molecule two circulating products are formed, the inactive intermediate form (ADM_{gly}) and the active mature form (ADM). Being a secreted product of the vascular endothelium along with NO and endothelin, ADM is largely distributed according to tissue vascularity.

ADM activates a combined calcitonin receptor-like receptor (CRLR) and the receptor activity modifying protein (RAMP2), possibly RAMP3, coupled receptor and increases the formation of intracellular

cAMP (12). The best-described effect of ADM is vasodilation, but the exact function in human physiology and pathophysiology, including up-regulation during inflammation, remains to be determined. In healthy volunteers, administered ADM dose-dependently decreases systolic and diastolic blood pressure (BP) and increases heart rate (HR) (13, 14). Facial flushing, conjunctival injection and mild headache have furthermore been described. Headache was observed in six of eight subjects and, respectively, in one out of 11 subjects (15, 16) after ADM administration.

ADM receptors are situated on the endothelial and smooth muscle cells of cerebral vessels and ADM is produced within cerebral endothelial cells, in contrast to CGRP, which is released from perivascular sensory nerve endings. CGRP does not seem to play an important role in the maintenance of resting tone of cerebral vessels (17), whereas ADM might do so at high plasma levels (11).

The properties of ADM and its similarity to CGRP, as well as the possible activation of CGRP receptors by ADM, make it an obvious candidate to be involved in migraine mechanisms. We therefore conducted this double-blind study to evaluate whether ADM affects the cerebral and extracranial haemodynamics and whether it causes headache or migraine in migraine suffers.

Methods and patients

Design and patients

A placebo-controlled, double-blind, crossover design was applied in the study. The number of patients ($n = 12$) to be included was estimated according to Pocock (18) and based on the following assumptions: the probability of inducing a migraine attack on active days was set at 0.5 and on placebo days to 0.1, to 5% and to 10%. Fourteen patients were included, but two were excluded due to development of claustrophobia during the baseline single-photon emission computed tomography (SPECT) scan. In all, 12 patients completed both treatment days.

The migraine patients all fulfilled the criteria of the International Headache Society (IHS) (19) for migraine without aura (MoA) and had a maximum of six attacks per month. A second diagnose of tension-type headache was allowed with a maximum of four episodes per month. Entry criteria were: MoA (19) and age 18–65 years. Exclusion criteria were: present or previous cardiovascular, cerebrovascular, endocrine or neurological disorder, prophylactic treatment for migraine and concomitant medication that might influence the outcome measures.

The study population consisted of 10 women and two men with a mean age of 41 years (range 28–50 years). Written informed consent was obtained before randomization. The Ethical Committee of Copenhagen (KA01115s) and the Danish Medicines Agency (2612-1771) approved the study, which was conducted according to the Helsinki II declaration. A balanced randomization was performed using Medstat©. A double-blind, crossover design was used. Placebo (0.9% NaCl) or human ADM (0.08 g kg ^{1} min ^{1}) was administered intravenously in a balanced randomized order on the two different trials days. h-ADM(1-52) was purchased from Clinalfa AG (Bubendorf, Switzerland) and diluted in 0.9% isotonic saline immediately before administration.

The choice of ADM dose was partly based on previously published studies using doses between 0.016 and 0.081 g kg ^{1} min ^{1} and partly on a dose finding pilot study including three patients suffering from MoA. In a single trial day they received three intravenous (i.v.) cumulative doses of ADM [0.06, 0.08 and 0.1 g kg ^{1} min ^{1} (i.v.)] as 20-min infusions separated by a 60-min wash-out period. The first patient developed severe tachycardia, increasing BP, peripheral vasoconstriction and cold sweating after the 0.1- g dose. Therefore, the two remaining patients received only 0.06 and 0.08 g kg ^{1} min ^{1} of ADM (i.v.), which was well tolerated.

Headache and adverse events

Every 10 min from baseline to T_{120} (end of study period) the patients were questioned for the presence of headache, associated symptoms and adverse events (AEs). Between questionings the patients self-reported any changes they might experience. The intensity of the AEs was graded as mild, moderate or severe and their relationship to ADM was classified as related or not related by the investigator. Headache intensity was scored on an 11-point verbal rating scale with 0 = no headache, 1 = mild headache or a sensation of pressing or throbbing inside the head, not necessarily felt as actual pain, 5 = medium severe headache, 10 = worst imaginable headache. Accompanying symptoms were recorded according to the IHS (19). After discharge, patients made an hourly recording of headache up to 24 h after the infusion of placebo or ADM.

Cerebral blood flow measurements

Global and regional cerebral blood flow (CBF) was measured with ^{133}Xenon inhalation and SPECT with a brain-dedicated camera (Ceraspect; DSI, Waltham, MA, USA). The apparatus consists of a stationary annular NaI crystal and a fast rotating collimator system. Each rotation took 10 s, thereby acquiring one frame in a 30-frame dynamic protocol of ^{133}Xenon inhalation, three background, nine wash-in, 18 wash-out using the Kanno-Lassen algorithm (20). A photoelectric window of 70–100 keV was employed.

Thirty-two slices were reconstructed in a 64 64 matrix with each pixel measuring 0.33 0.33 cm using a Butterworth 1D filter (cut-off 1.5, order 6). The 32 slices were reduced to sets of eight transaxial slices generated by adding four slices together to a total slice thickness of 1.32 cm. Attenuation correction using the Chang algorithm (= 0.05 cm) and correction for nose artefact was performed. The output for each pixel was the k_i-value and flow values were estimated from these using the partition coefficient ( ) of 0.85 ml/g (grey matter).

A Datex Normocap 200 (Dameca, Roedovre, Denmark) was used for end-tidal CO_2 measurements during the CBF acquisitions. A Ceratronic XAS SM 320 (Randers, Denmark) was used for the ^{133}Xenon administration. Each measurement lasted 5 min.

Calculations of flow in the perfusion territories of the major cerebral arteries were performed fitting standard vascular regions of interest on the five slices at 3.6, 5.0, 6.3, 7.6 and 9 cm above the orbitomeatal line. Flow in the territory of the middle cerebral artery (MCA) ($rCBF_{MCA}$) was calculated as a mean of the left and right side.

Transcranial Doppler and C-scan

Transcranial Doppler (TCD) ultrasonography (2 MHz, Multidop X Doppler; DWL, Sipplingen, Germany) was used for the measurement of blood flow velocity. The recordings were done simultaneously and bilaterally as previously described, but with handheld probes (21). Along the MCA, a fixed point was found for the measurement. The fixed point was chosen as close as possible to the bifurcation of the anterior cerebral artery and MCA. The same fix-point was used for each individual and for each recording, at which the signal was optimized. Based upon the envelope curve (spectral TCD curve), a time-average mean (V_{mean}) over approximately four cardiac cycles (4 s) was calculated by the built-in software (TCD software for MDX 7.40x). The final measure used for each time point was an average of four cycles (V_{MCA}). Simultaneously with the TCD recording, a mask covering the subjects' mouth and nose region was placed for the measurement of end-tidal pCO_2 ($P_{et}CO_2$) (Datex Normocap 200; Dameca).

A high-resolution ultrasound scanner, C-scan (Dermascan C, 20 MHz, bandwidth 15 MHz; Hadsund, Denmark) was used to measure the diameter of the left temporal and left radial arteries (22). The diameter of the former was measured at the front branch of the superficial temporal artery (STA) and the latter at the wrist. To ensure that the repeated measurements with TCD and C-scan were performed in the same place, marks were drawn on the skin. After the last recording on the first trial day, the coordinates of the marks were recorded for re-use on the following trial day.

Pharmacokinetics

At the beginning of each trial day the haematocrit value was determined. Plasma samples for the analysis of ADM concentration (ADM_{Total} and ADM_{Mature}) were obtained four times during each trial day (T_{20}, $T_{19.5}$, T_{60} and T_{120}). The plasma samples were collected in cooled 10-ml K3 ethylenediamine tetraaceticacid vacutainers containing Apropotinin (Trasylol© 0.6 antecubital unit/ml blood) from the cubital vein contralateral to the site of ADM or placebo infusion. The samples were immediately placed on ice and subsequently centrifuged for 10 min (1500 *g*) at 4°C. Plasma was stored at 30°C until analysed at the University of Miyazaki, Japan. The applied assay for measurement of ADM has previously been validated (23, 24).

Trial procedures

The migraine patients began the study at 07.45 h with a short interview ensuring the following inclusion criteria: no migraine attack or tension-type headache for the preceding 48 h, no intake of triptans or analgesics, e.g. paracetamol, within the same period of time, no intake of ergotamine for the previous 72 h and abstinence from coffee, tea, caffeine-containing drinks and smoking tobacco for the preceding 8 h. The patients rested supine throughout the study period.

Two i.v. catheters [Optiva*2, (18G); Johnson & Johnson, Ethicon S.p.A., Italy] were inserted into the cubital veins, one for the administration of

placebo or h-ADM, the other for blood sampling. The volunteers rested at least 30 min before baseline values of CBF, V_{MCA}, temporal and radial diameter, BP, HR and electrocardiogram (ECG) were recorded. The start of infusion of h-ADM or placebo was designated time zero (T_0). The infusion lasted 20 min and was administered by a time- and volume-controlled infusion pump (Braun® perfusor; B. Braun, Melsungen, Germany).

The SPECT measurements were repeated twice at T_{25} and T_{115}. Every 10 min from T_{20} until T_{120} questioning for headache and associated symptoms followed by measurement of TCD and C-scans were performed. BP, HR (Omega 1400; In vivo Research Laboratories Inc., Copiague, NY, USA) and ECG (Cardiofax; Nihon Kohden Corp., Tokyo, Japan) were recorded at T_{20}, T_{10}, T_0 and thereafter every 5 min throughout the study.

$rCBF_x$ in the area of a given artery (x) is related to mean blood flow velocity ($V_{mean(x)}$) and cross-sectional area, r^2, of the artery.

$$rCBF_{(x)} = V_{mean(x)} \times \pi \times r^2$$

If the rCBF changes the following equation is valid:

$$\Delta Diameter = \left(\left(\sqrt{\frac{rCBF_{2(x)}/Vmean_{2(x)}}{rCBF_{1(x)}/Vmean_{1(x)}}}\right) - 1\right) \times 100$$

Diameter is the relative percent change in diameter; $V_{mean1(x)}$ is the mean blood velocity before infusion of drugs and $V_{mean2(X)}$ the velocity at a relevant time point after the infusion. The same nomination is applied for rCBF (25, 26).

Statistics

Baseline was calculated as a mean of the values at T_{20}, T_{10} and T_0. Values are presented as means ± S.D. $P < 0.05$ was considered significant. All analyses were performed using SPSS statistical software version 10.0 (SPSS Inc., Chicago, IL, USA).

For changes over time on each trial day global CBF, $rCBF_{MCA}$, V_{MCA}, diameter of the temporal and radial artery, BP, HR and $P_{et}CO_2$ were analysed by univariate analysis of variance for the factors time and subject. If a significant change was found, a *post hoc* analysis (Dunnett's multiple comparisons test) was performed to localize the change. To eliminate the risk of mass significance on measurements with numerous repeated measurements, four points of interest were chosen: baseline, 20 min, 60 min and 120 min. Absolute values were used for the statistical analysis. For the comparison between ADM and placebo a paired *t*-test was performed for the following measurements: global CBF, $rCBF_{MCA}$, V_{MCA}, diameter of the temporal and radial artery, BP, HR and $P_{et}CO_2$. Summary measure for the *t*-test was the area under the curve (AUC) calculated on percentage changes from baseline.

Immediate headache was defined as any headache during the first 60 min after the start of the h-ADM administration. Any headache occurring thereafter was called delayed headache. Peak values and $AUC_{Headache}$ (area under the headache curve) were compared between the two trial days using Wilcoxon's signed rank test. The occurrence of headache and AEs on the two trial days was compared with McNemar's test.

Results

Baseline characteristics

No significant differences were found between the two experimental days in values of haemodynamic variables, haematocrit or start and end room temperature.

Headache and associated symptoms

Of the 12 included patients, six experienced immediate headache on days with administration of ADM and one on placebo days ($P = 0.13$). Four patients had a delayed headache on placebo days and seven after ADM ($P = 0.38$). Figure 1 shows the headache score of the individual patients. Analysis of the peak headache revealed no difference between ADM and placebo for the immediate ($P = 0.17$) or delayed ($P = 0.87$) period. Based on the $AUC_{Headache}$, a tendency towards difference in the immediate period was found ($P = 0.051$), but none was detected for the entire registration ($P = 0.58$) or delayed period ($P = 0.78$). The experienced headache fulfilled the IHS criteria for MoA in six cases. Two patients had MoA on both trial days, and in the remaining four patients two after ADM and two after placebo administration.

ADM induced flushing in all patients and placebo in one ($P = 0.001$), 11 patients experienced heat sensation after ADM and four after placebo ($P = 0.016$).

Pharmacokinetics

Baseline plasma concentration of ADM_{total} (11.67 ± 2.43 fmol/ml and 11.09 ± 2.7 fmol/ml) and ADM_{mature} (2.78 ± 0.68 fmol/ml and 2.77 ± 0.58 fmol/ml) were similar on the two trial days.

The C_{max} of ADM_{total} (76.4 ± 16.6 fmol/ml) and ADM_{mature} (24.4 ± 6.0 fmol/ml) were measured at time point $T_{19.5}$, at the end of the h-ADM infusion. After 2 h the plasma levels had not yet returned to baseline (Fig. 2). On placebo days no change from the baseline values were recorded.

Cerebral and peripheral haemodynamics

There were no significant differences in baseline values between ADM and placebo administration days (Table 1). After ADM there was no change in global CBF ($P = 0.32$ $P_{et}CO_2$ uncorrected, and $P = 0.22$ $P_{et}CO_2$ corrected) or in $rCBF_{MCA}$ ($P = 0.38$, $P_{et}CO_2$ uncorrected, and $P = 0.27$ $P_{et}CO_2$ corrected) compared with placebo (Fig. 3). Global CBF and $rCBF_{MCA}$ increased significantly ($P = 0.034$ and $P = 0.035$) over time after ADM when the measurements were corrected for $P_{et}CO_2$. The increase was only seen 5 min after termination of the infusion. However, without $P_{et}CO_2$ correction no significant increase was seen ($P = 0.097$ and $P = 0.096$). On placebo days no change over time was seen. $P_{et}CO_2$ measured during CBF acquisition did not change over time, and there was no difference between treatments ($P = 0.32$).

$P_{et}CO_2$-corrected V_{MCA} increased significantly over time after ADM ($P = 0.027$). The difference from baseline was recorded at time point T_{20} and was 6.6 ± 2.4%. For the left MCA alone ($V_{MCA(left)}$) a similar result was obtained ($P = 0.023$). The right

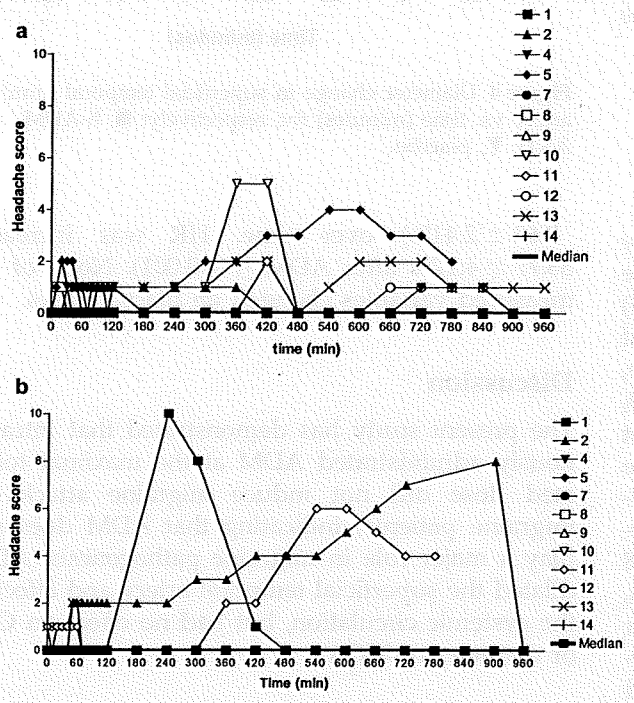

Figure 1 Individual curves of headache scores for all patients on days of h-ADM infusion (a) and placebo (b). The median headache score is in bold.

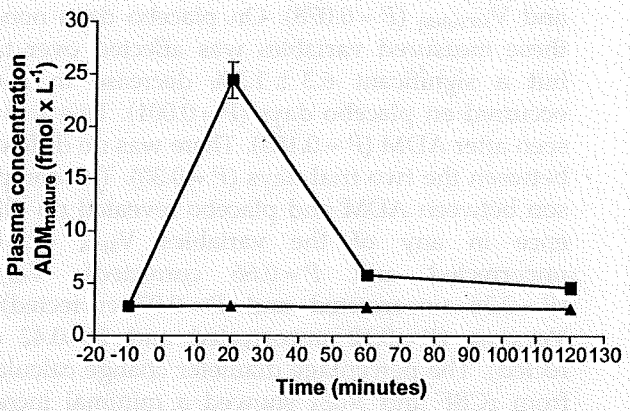

Figure 2 Plasma concentration of ADM_{Mature} on the two trial days; ■, h-ADM; ▼, placebo.

Table 1 Baseline values on the two trial days with comparison using a paired *t*-test

	Adrenomedullin		Placebo		
	Mean	(±) S.D.	Mean	(±) S.D.	*P*
$V_{MCA\ left}$ (cm/s)	74.74	13.15	78.92	13.32	0.085
$V_{MCA\ right}$ (cm/s)	77.66	11.84	81.49	13.81	0.171
$V_{MCA\ mean}$ (cm/s)	76.20	11.36	80.20	12.86	0.081
pCO_2 (mmHg)	36.75	4.29	37.75	4.61	0.255
Radial artery (mm)	2.35	0.52	2.36	0.56	0.965
Temporal artery (mm)	1.11	0.28	1.09	0.19	0.791
Systolic BP (mmHg)	116.94	11.82	116.17	13.62	0.724
Diastolic BP (mmHg)	72.42	8.00	73.08	8.95	0.780
Mean BP (mmHg)	86.90	8.40	88.03	10.62	0.618
Heart rate (bpm)	61.01	9.45	61.75	7.84	0.639

BP, blood pressure.

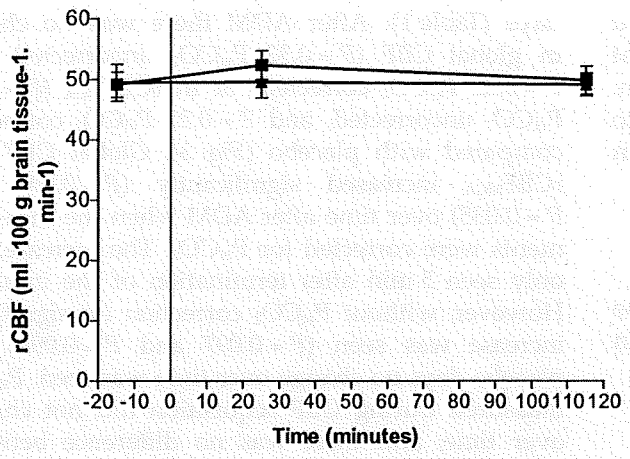

Figure 3 rCBF (ml 100 g brain tissue ^{1} min ^{1}) vs. time (minutes) for, respectively: ■, h-ADM administered; ▼, placebo. Vertical line = initiation of infusion.

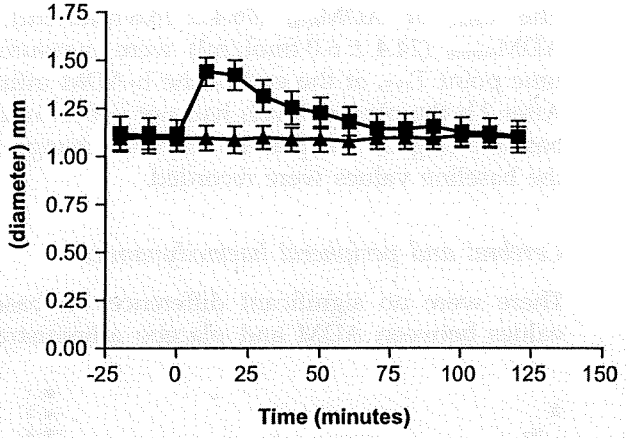

Figure 4 Diameter change in superficial temporal (mm) artery vs. time (minutes) for, respectively: ■, h-ADM AND; ▼, placebo.

MCA ($V_{MCA(right)}$) was not significantly affected by the ADM. Without $P_{et}CO_2$ correction, none of the significant increases was observed, V_{MCA} ($P = 0.069$) and $V_{MCA(left)}$ ($P = 0.078$). On placebo days none of these measured variables was affected over time, but a significant $6.3 \pm 1.5\%$ decrease in $P_{et}CO_2$ occurred on placebo days ($P = 0.001$). This was not seen after ADM ($P = 0.155$). There was no difference between the two trial days ($P = 0.30$). The comparison between ADM and placebo revealed no difference in any of the variables V_{MCA} ($P = 0.18$ uncorrected and $P = 0.66$ corrected), $V_{MCA(left)}$ ($P = 0.36$ uncorrected and $P = 0.97$ corrected) or $V_{MCA(right)}$ ($P = 0.12$ uncorrected and $P = 0.42$ corrected). The percentage diameter change calculated from rCBF and V_{MCA} showed a minimal increase ($1.2\% \pm 3.5\%$) at T_{25} after ADM, and there was no difference between trial days ($P = 0.72$).

Temporal artery diameter increased significantly compared with placebo ($P = 0.01$), whereas the radial artery diameter was unchanged after ADM compared with placebo ($P = 0.38$). ADM increased the temporal artery diameter over time ($P < 0.001$), the maximal increase being recorded at T_{10} and $33.42 \pm 6.22\%$. The temporal ($P = 0.47$) and radial artery diameter ($P = 0.53$) was unaffected over time after placebo, as was the radial diameter after ADM ($P = 0.21$) (Fig. 4).

There were no significant changes after ADM compared with placebo in systolic BP ($P = 0.23$), diastolic BP ($P = 0.9$) or mean BP ($P = 0.86$). HR was significantly increased after ADM ($P = 0.003$) compared with placebo. ADM induced a significant decrease in systolic BP ($P = 0.03$), diastolic BP ($P < 0.001$, $9.53 \pm 1.93\%$) and mean BP ($P < 0.001$, $7.63 \pm 2.41\%$) over time. HR was increased $33.77 \pm 4.17\%$ after ADM ($P < 0.001$). None of the measured variables changed on placebo days.

Discussion

The present study has demonstrated that intravenously administrated ADM at the maximal tolerated dose did not induce migraine attacks in migraine patients, indicating that ADM does not play a major role in migraine pathogenesis. ADM dilated the superficial temporal artery and affected the systemic circulation, but had no effect on CBF or diameter of MCA.

Haemodynamic effects of ADM

Meeran and co-workers administered ADM to healthy volunteers and found that a low dose of ADM (3.2 pmol kg ^{1} min ^{1}) did not affect BP or HR, whereas a higher dose (13.4 pmol kg ^{1} min ^{1}) resulted in a significant decrease in diastolic BP (69 ± 2 to 53 ± 2 mmHg) and a significant increase in HR (57 ± 3 to 95 ± 4 bpm) (13). With a dose of 0.05 g kg ^{1} min ^{1} Nagaya et al. found smaller effects, but a significantly increased cardiac index and decreased pulmonary arterial pressure in patients with chronic heart failure (15). Long-term administration of AM in lower doses (2.9 and 5.8 pmol kg ^{1} min ^{1}) showed a minor effect on systemic haemodynamics (14, 16). Administering 0.08 g kg ^{1} min ^{1} for 20 min, we found that the systolic, diastolic and mean arterial BP were unaffected by ADM compared with placebo. HR was significantly increased.

The effect of ADM on human CBF or MCA diameter has not been assessed previously. Data on endogenous production within the brain are conflicting. It seems likely that cerebral endothelial cells produce a high amount of ADM (10, 27, 28). ADM has been shown to pass the blood–brain barrier (BBB) and may be involved in the regulation of BBB function (29, 30). Since ADM receptors are present on both endothelial and vascular smooth muscle cells and possess vasodilatory properties, one would expect ADM to be a strong cerebral vasodilator. However, we found no significant effect on CBF or MCA diameter. This finding contrasts with animal studies, which have all shown vasodilation and increase in CBF. Species differences may partly explain the findings. Thus, the expression of functional ADM receptors might differ between humans and rodents, and the physiological role of ADM is more likely to be regulation of BBB permeability than vasodilation (30–32).

The infusion of ADM resulted in a significant dilation of the superficial branch of the temporal artery compared with placebo. This dilation seemed to be restricted to the cephalic circulation since no effect was seen on the radial (control) artery. The dilation was associated with a concomitant flushing of the face and chest in all but one patient, and a sensation of heat was an often-reported side-effect of the ADM infusion.

Extracranial arterial dilation causes no headache

ADM did not induce a migraine headache in our study population despite its close relation to CGRP and its vasodilatory properties. A possible cause of the failure of ADM to induce migraine headache could be that the dose of ADM was too low. However, plasma ADM_{total} (ADM_{gly} + ADM_{mature}) increased 6.5 times and ADM_{mature} 8.8 times. In patients with an altered cerebral circulation after subarachnoid haemorrhage only a four-times increase in ADM plasma concentrations was measured (33). Furthermore, the infusion of a higher dose in the pilot study induced a substantial effect on BP and HR and was deemed unsuitable. We therefore feel confident that the administered dose of ADM was sufficient to induce migraine if the peptide was indeed a mediator of migraine.

Our human model of experimental headache has demonstrated its ability to describe the headache/migraine-inducing potential of several substances, e.g. NO, CGRP and histamine (2, 34, 35). In healthy individuals this headache is monophasic, occurring during and shortly after the infusion. The experimentally induced headache in migraine patients is characterized by a biphasic course with an immediate headache, often similar to the headache experienced by non-migraineurs, and a delayed headache occurring between 1 and 12 h later. The delayed headache fulfilled criteria for MoA in three out of nine patients after CGRP administration (2), in five out of 12 after histamine (36) and in approximately 80% after GTN. In previous studies both intracranial and extracranial dilation were seen, and in spontaneous migraine attacks both the MCA and STA were dilated (37, 38). It remains uncertain which of these territories is most important for migraine induction (39). ADM is the first substance shown to dilate STA without affecting MCA or CBF. Our results indicate that dilation of extracranial vessels is not enough of itself to induce migraine.

In conclusion, the infusion of ADM failed to induce headache or migraine in migraine patients, compared to placebo. It is therefore unlikely that ADM plays a pivotal role in migraine pathogenesis. The vasodilatory properties of ADM were confirmed for the STA and extracranial arterioles (flushing), but neither the MCA diameter nor CBF changed.

Acknowledgements

The technical equipment used was partly sponsored by The Villum Kann Rasmussen Foundation and The Toyota Foundation. The Lundbeck Foundation funds the research of the Danish Headache Centre. Special thanks to Lene Elkjær and Kirsten Bruunsgaard for excellent technical support.

References

1 Goadsby PJ, Edvinsson L, Ekman R. Vasoactive peptide release in the extracerebral circulation of humans during migraine headache. Ann Neurol 1990; 28:183–7.
2 Lassen LH, Haderslev PA, Jacobsen VB, Iversen HK, Sperling B, Olesen J. CGRP may play a causative role in migraine. Cephalalgia 2002; 22:54–61.
3 Olesen J, Diener HC, Husstedt IW, Goadsby PJ, Hall D, Meier U et al. Calcitonin gene-related peptide receptor antagonist BIBN 4096 BS for the acute treatment of migraine. N Engl J Med 2004; 350:1104–10.
4 Petersen KA, Lassen LH, Birk S, Lesko L, Olesen J. BIBN4096BS antagonizes human alpha-calcitonin gene related peptide-induced headache and extracerebral artery dilatation. Clin Pharmacol Ther 2005; 77:202–13.
5 Thomsen L, Kruuse C, Iversen H, Olesen J. A nitric donor (nitroglycerin) triggers genuine migraine attacks. Eur J Neurol 1994; 1:73–80.
6 Wei EP, Moskowitz MA, Boccalini P, Kontos HA. Calcitonin gene-related peptide mediates nitroglycerin and sodium nitroprusside-induced vasodilation in feline cerebral arterioles. Circ Res 1992; 70:1313–19.

7 Kitamura K, Kangawa K, Kawamoto M, Ichiki Y, Nakamura S, Matsuo H et al. Adrenomedullin: a novel hypotensive peptide isolated from human pheochromocytoma. Biochem Biophys Res Commun 1993; 192:553–60.

8 Hinson JP, Kapas S, Smith DM. Adrenomedullin, a multifunctional regulatory peptide. Endocr Rev 2000; 21:138–67.

9 Ishimitsu T, Kojima M, Kangawa K, Hino J, Matsuoka H, Kitamura K et al. Genomic structure of human adrenomedullin gene. Biochem Biophys Res Commun 1994; 203:631–9.

10 Kis B, Kaiya H, Nishi R, Deli MA, Abraham CS, Yanagita T et al. Cerebral endothelial cells are a major source of adrenomedullin. J Neuroendocrinol 2002; 14:283–93.

11 Kis B, Abraham CS, Deli MA, Kobayashi H, Wada A, Niwa M et al. Adrenomedullin in the cerebral circulation. Peptides 2001; 22:1825–34.

12 McLatchie LM, Fraser NJ, Main MJ, Wise A, Brown J, Thompson N et al. RAMPs regulate the transport and ligand specificity of the calcitonin- receptor-like receptor. Nature 1998; 393:333–9.

13 Meeran K, O'Shea D, Upton PD, Small CJ, Ghatei MA, Byfield PH et al. Circulating adrenomedullin does not regulate systemic blood pressure but increases plasma prolactin after intravenous infusion in humans: a pharmacokinetic study. J Clin Endocrinol Metab 1997; 82:95–100.

14 Lainchbury JG, Troughton RW, Lewis LK, Yandle TG, Richards AM, Nicholls MG. Hemodynamic, hormonal, and renal effects of short-term adrenomedullin infusion in healthy volunteers. J Clin Endocrinol Metab 2000; 85:1016–20.

15 Nagaya N, Nishikimi T, Uematsu M, Satoh T, Oya H, Kyotani S et al. Haemodynamic and hormonal effects of adrenomedullin in patients with pulmonary hypertension [In Process Citation]. Heart 2000; 84:653–8.

16 Troughton RW, Lewis LK, Yandle TG, Richards AM, Nicholls MG. Hemodynamic, hormone, and urinary effects of adrenomedullin infusion in essential hypertension [In Process Citation]. Hypertension 2000; 36:588–93.

17 Petersen KA, Birk S, Lassen LH, Kruuse C, Jonassen O, Lesko L et al. The CGRP-antagonist, BIBN4096BS does not affect cerebral or systemic haemodynamics in healthy volunteers. Cephalalgia 2005; 25:139–47.

18 Pocock SJ. Clinical trials: a practical approach. New York: John Wiley & Sons 1983.

19 Headache Classification Committee of the International Headache Society. Classification and diagnostic criteria for headache disorders, cranial neuralgias and facial pain. Cephalalgia 1988; 8 (Suppl. 7):1–96.

20 Kanno I, Lassen NA. Two methods for calculating regional cerebral blood flow from emission computed tomography of inert gas concentrations. J Comput Assist Tomogr 1979; 3:71–6.

21 Thomsen LL, Iversen HK. Experimental and biological variation of three-dimensional transcranial Doppler measurements. J Appl Physiol 1993; 75:2805–10.

22 Nielsen TH, Iversen HK, Tfelt-Hansen P. Determination of the luminal diameter of the radial artery in man by high frequency ultrasound: a methodological study. Ultrasound Med Biol 1990; 16:787–91.

23 Ohta H, Tsuji T, Asai S, Sasakura K, Teraoka H, Kitamura K et al. One-step direct assay for mature-type adrenomedullin with monoclonal antibodies. Clin Chem 1999; 45:244–51.

24 Ohta H, Tsuji T, Asai S, Tanizaki S, Sasakura K, Teraoka H et al. A simple immunoradiometric assay for measuring the entire molecules of adrenomedullin in human plasma. Clin Chim Acta 1999; 287:131–43.

25 Dahl A, Russell D, Nyberg-Hansen R, Rootwelt K. Effect of nitroglycerin on cerebral circulation measured by transcranial Doppler and SPECT. Stroke 1989; 20:1733–6.

26 Sorteberg W. Cerebral artery velocity and cerebral blood flow. In: Newell DW, Aaslid R, eds. Transcranial doppler. New York: Raven Press Ltd 1992:57–66.

27 Ladoux A, Frelin C. Coordinated up-regulation by hypoxia of adrenomedullin and one of its putative receptors (RDC-1) in cells of the rat blood–brain barrier. J Biol Chem 2000; 275:39914–19.

28 Sugo S, Minamino N, Kangawa K, Miyamoto K, Kitamura K, Sakata J et al. Endothelial cells actively synthesize and secrete adrenomedullin. Biochem Biophys Res Commun 1994; 201:1160–6.

29 Kastin AJ, Akerstrom V, Hackler L, Pan W. Adrenomedullin and the blood–brain barrier. Horm Metab Res 2001; 33:19–25.

30 Kis B, Deli MA, Kobayashi H, Abraham CS, Yanagita T, Kaiya H et al. Adrenomedullin regulates blood–brain barrier functions *in vitro*. Neuroreport 2001; 12:4139–42.

31 Kis B, Abraham CS, Deli MA, Kobayashi H, Niwa M, Yamashita H et al. Adrenomedullin, an autocrine mediator of blood–brain barrier function. Hypertens Res 2003; 26 (Suppl.):S61–70.

32 Kis B, Snipes JA, Deli MA, Abraham CS, Yamashita H, Ueta Y et al. Chronic adrenomedullin treatment improves blood–brain barrier function but has no effects on expression of tight junction proteins. Acta Neurochir Suppl 2003; 86:565–8.

33 Kikumoto K, Kubo A, Hayashi Y, Minamino N, Inoue S, Dohi K et al. Increased plasma concentration of adrenomedullin in patients with subarachnoid hemorrhage. Anesth Analg 1998; 87:859–63.

34 Iversen HK, Olesen J, Tfelt-Hansen P. Intravenous nitroglycerin as an experimental model of vascular headache. Basic characteristics. Pain 1989; 38:17–24.

35 Lassen LH. Histamine induced headache. Possible involvement of nitric oxide. [PhD]. Glostrup: University of Copenhagen 1997.

36 Lassen LH, Christiansen I, Iversen HK, Jansen-Olesen I, Olesen J. The effect of nitric oxide synthase inhibition on histamine induced headache and arterial dilatation in migraineurs. Cephalalgia 2003; 23:877–86.

37 Iversen HK, Nielsen TH, Olesen J, Tfelt-Hansen P. Arterial responses during migraine headache. Lancet 1990; 336:837–9.

38 Thomsen LL, Iversen HK, Olesen J. Cerebral blood flow velocities are reduced during attacks of unilateral migraine without aura. Cephalalgia 1995; 15:109–16.

39 Olesen J, Tfelt-Hansen P, Welch K. The headaches. Philadelphia: Lippincott Williams and Wilkins 2000.

Am J Physiol Heart Circ Physiol 297: H1274–H1280, 2009.
First published August 14, 2009; doi:10.1152/ajpheart.00503.2009.

Pharmacological stimulation of soluble guanylate cyclase modulates hypoxia-inducible factor-1α in rat heart

Toshihiro Tsuruda,[1] Kinta Hatakeyama,[2] Hiroyuki Masuyama,[1] Yoko Sekita,[1] Takuroh Imamura,[1] Yujiro Asada,[2] and Kazuo Kitamura[1]

[1]*Faculty of Medicine, Department of Internal Medicine, Circulatory and Body Fluid Regulation, and* [2]*Department of Pathology, University of Miyazaki, Miyazaki, Japan*

Submitted 3 June 2009; accepted in final form 13 August 2009

Tsuruda T, Hatakeyama K, Masuyama H, Sekita Y, Imamura T, Asada Y, Kitamura K. Pharmacological stimulation of soluble guanylate cyclase modulates hypoxia-inducible factor-1α in rat heart. *Am J Physiol Heart Circ Physiol* 297: H1274–H1280, 2009. First published August 14, 2009; doi:10.1152/ajpheart.00503.2009.—Mechanical load and ischemia induce a series of adaptive physiological responses by activating the expression of O_2-regulated genes, such as hypoxia inducible factor-1α (HIF-1α). The aim of this study was to explore the interaction between HIF-1α and soluble guanylate cyclase (sGC) and its second messenger cGMP in cultured cardiomyocytes exposed to hypoxia and in pressure-overloaded heart. In cultured cardiomyocytes of neonatal rats, either sGC stimulator BAY 41-2272 or cGMP analog 8-bromo-cGMP decreased the hypoxia (1% O_2/5% CO_2)-induced HIF-1α expression, whereas the inhibition of protein kinase G by KT-5823 reversed the effect of BAY 41-2272 on the expression under hypoxic conditions. In pressure-overloaded heart induced by suprarenal aortic constriction (AC) in 7-wk-old male Wistar rats, the administration of BAY 41-2272 (2 $mg \cdot kg^{-1} \cdot day^{-1}$) for 14 days significantly suppressed the protein expression of HIF-1α ($P < 0.05$), vascular endothelial growth factor ($P < 0.01$), and the number of capillary vessels ($P < 0.01$) induced by pressure overload. This study suggests that the pharmacological sGC-cGMP stimulation modulates the HIF-1α expression in response to hypoxia or mechanical load in the heart.

cyclic guanosine monophosphate; hypoxia; mechanical load; angiogenesis; inflammation

THE MYOCARDIUM IS AN elastic network of cardiomyocytes enmeshed in a collagen matrix that connects the myocytes and supporting intramyocardial coronary vasculature. Mechanical load or ischemia induces a series of adaptive physiological responses in the heart [cardiomyocyte hypertrophy, interstitial fibrosis, and angiogenesis (24, 29)]. Hypoxia inducible factor-1 (HIF-1) is one of the most important transcription factors, composed of following subunits: a constitutively expressed HIF-1β and HIF-1α induced by hypoxia, and the latter subunit induces the expression of a number of downstream genes, including that for the vascular endothelial growth factor (VEGF) (26). Expressions of HIF-1α and VEGF are reported to be activated in hypertrophied and failing heart (17, 26, 29, 30), and the increased number of capillary vessels penetrating the interstitial spaces contribute to supply oxygen and nutrients to the cardiocytes for maintaining the structure and function of pressure-overloaded heart (29, 34).

Address for reprint requests and other correspondence: T. Tsuruda, Dept. of Internal Medicine, Circulatory and Body Fluid Regulation, Faculty of Medicine, Univ. of Miyazaki, 5200 Kihara Kiyotake, Miyazaki 889-1692, Japan (e-mail: ttsuruda@med.miyazaki-u.ac.jp).

Guanylate cyclase is an enzyme that converts guanosine triphosphate to cyclic guanosine monophosphate (cGMP). Soluble guanylate cyclase (sGC) activated by nitric oxide has been shown to attenuate cardiovascular remodeling by elevating intracellular cGMP levels (6, 18). We and others have previously reported that the pharmacological stimulation of sGC with BAY 41-2272 attenuated the adverse remodeling associated with systemic or pulmonary hypertension, suggesting that sGC-cGMP activation would be one of the important therapeutic targets for the treatment in the disorders (7, 22, 23). However, the interaction between sGC-cGMP signaling and HIF-1α expression during mechanical load/ischemia in the heart is unknown. Therefore, we sought to examine whether the pharmacological stimulation of sGC-cGMP would affect the HIF-1α-angiogenic pathway in cultured cardiomyocytes exposed to hypoxia and in pressure-overloaded heart.

MATERIALS AND METHODS

The present study was performed in accordance with the Animal Welfare Act and with approval of the University of Miyazaki Institutional Animal Care and Use Committee (2006-014-3, 2002-049-7). It also conformed with the Guide for the Care and Use of Laboratory Animals published by the United States National Institutes of Health (NIH publication no. 85-23, revised 1996).

Cell culture. Cardiomyocytes were isolated from 1-day-old neonatal Wistar rats as described (38). The cardiomyocytes were cultured on collagen type I-coated culture plates for 48 h with DMEM containing 15 mmol/l HEPES, 10% FBS, 10 μg/ml insulin, 5 μg/ml transferrin, 7 ng/ml sodium selenite, and 0.1 mmol/l bromodeoxyuridine (BrdU) at 37°C in a humidified atmosphere of 95% air-5% CO_2 and further incubated in serum-free DMEM containing the same additives with the exception of BrdU for 48 h. The cells were cultured under normoxic (20% O_2-5% CO_2) or hypoxic (1% O_2-5% CO_2) conditions with or without 5×10^{-5} mol/l BAY 41-2272, a nonhydrolyzable cGMP analog (8-bromo-cGMP, 10^{-3} mol/l; Calbiochem), and a selective protein kinase G inhibitor (KT-5823, 10^{-6} mol/l; Calbiochem) that was added to the culture medium 30 min before hypoxia or BAY 41-2272. Specificity of BAY 41-2272 on concentration-dependent sGC stimulation has been addressed (33), whereas this compound does not stimulate particulate guanylate, adenylate cyclase, or phosphodiesterase 1, 2, 3, 4, 5, 6, 7, 8, 9, 10, and 11 [unpublished data, personal communication to Dr. Johannes-Peter Stasch, Bayer Schering Pharma (2, 39)]. The concentrations of 8-bromo-cGMP and KT-5823 were determined by reflecting in accordance with previous studies (14, 35, 41). After the cells had been cultured under normoxic or hypoxic conditions for 8 h, the nuclear extract was extracted according to the manufacturer's recommendations (Pierce). In addition, cultured cardiomyocytes treated with or without BAY 41-2272 for 10 min under normoxia were immediately collected for the cGMP assay as described previously (22).

Animal experiment. Male Wistar rats (7 wk old; Charles River) weighing 200–250 g were housed in a temperature- and light-controlled room (25 ± 1°C; 12:12-h light-dark cycle) for 1 wk before use, with free access to normal rat chow and water. The rats were divided into the following three groups: a sham group (n = 26) and two pressure-overloaded groups with (n = 36) or without (n = 58) BAY 41-2272 treatment. Pressure overload was induced by abdominal aortic constriction (AC) at the suprarenal level as previously described (10, 23). In brief, a 22-gauge needle was placed adjacent to the abdominal aorta proximal to the renal artery and ligated tightly around the aorta and the adjacent needle. The needle was then removed, leaving the vessel constricted to the diameter of the needle. The sham group underwent identical surgical procedures but without constriction of the aorta. The BAY 41-2272 compound, supplied by Bayer HealthCare, was given by gastric gavage at a dose of 2 mg/kg two times a day for 14 days. The dose of BAY 41-2272 was chosen according to our previous study (22, 23), in which 2 mg/kg was the subdepressor dose. The Datascience telemetric system was used to monitor the blood pressure and heart rate of four unrestricted, conscious rats in each study group, as described (23). On *day 14*, the survived rats were anesthetized with pentobarbital sodium and killed by drawing blood from the thoracic aorta. After the whole heart and lung were weighed, left ventricle (LV) was frozen in liquid nitrogen or fixed in 4% paraformaldehyde and embedded in paraffin wax.

Immunohistochemistry and histological analysis. Immunohistochemical staining with HIF-1α, von Willebrand factor (vWF) and monocyte/macrophages (CD68) was performed as reported (22, 36, 37). Tissue sections 3 μm thick fixed in 4% paraformaldehyde were pretreated before incubation with the primary antibodies: HIF-1α, autoclaved at 121°C for 15 min; vWF, covered with proteinase K at 37°C for 15 min; CD68, covered with 0.05% pronase at 37°C for 10 min. Slides were stained with antibodies of HIF-1α (1:6,000, clone H1alpha67; Novus Biologicals), vWF (1:100; DAKOcytometion) or CD68 (1:600, Clone ED1; Chemicon) overnight at 4°C. The slide sections were then incubated with EnVision$^+$ (DAKO) for 30 min, visualized with 0.05% 3,3′-diaminobenzidine containing hydrogen peroxide, and counterstained with hematoxylin. A catalyzed signal amplification system (CSA-DakoCytomation) was used for detecting HIF-1α antigen. Numbers of nuclei stained with HIF-1α, capillary vessels stained with vWF, or monocyte/macrophages stained with CD68 were counted at magnifications of ×200 in a blinded manner.

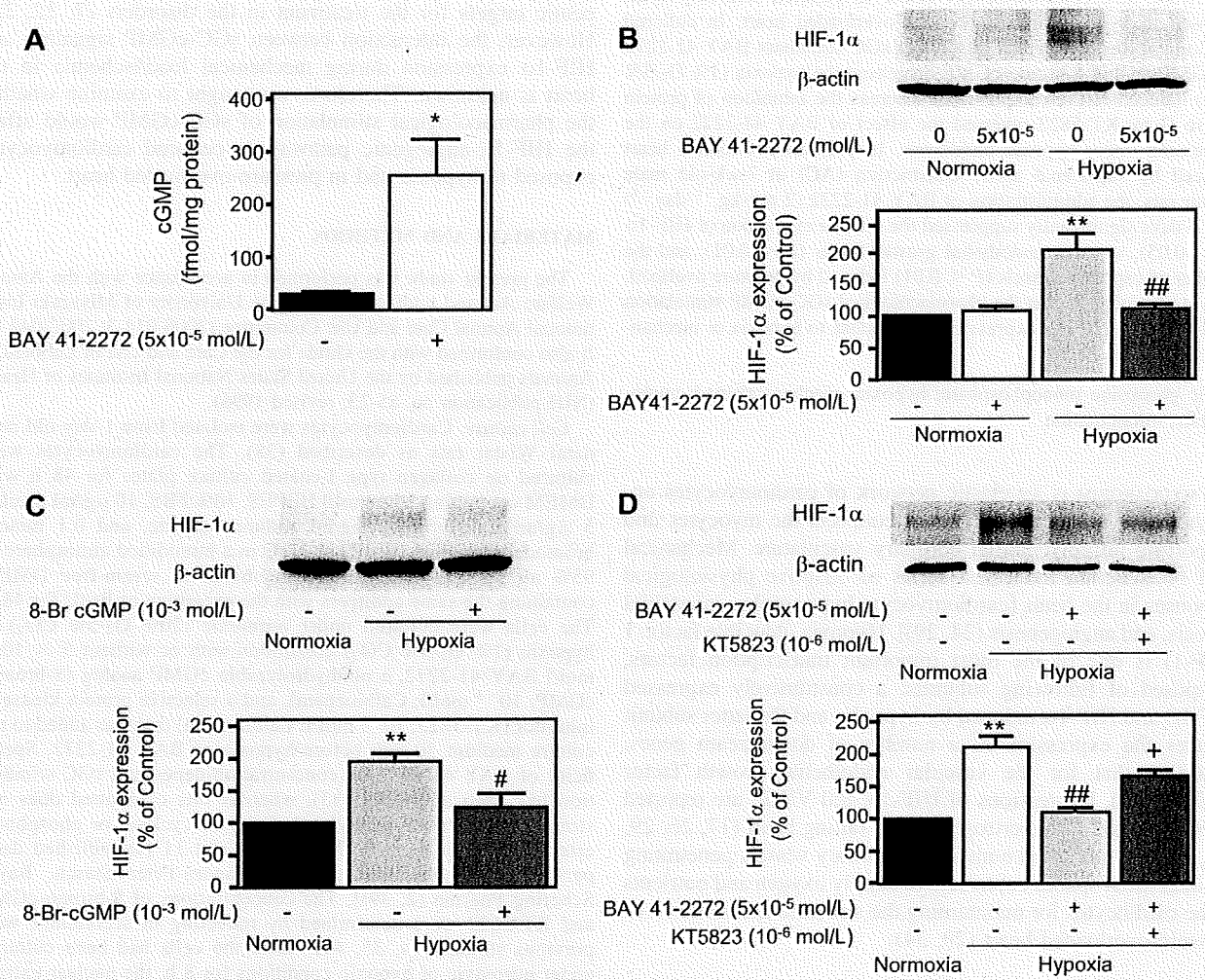

Fig. 1. *A*: Intracellular cGMP content after 10 min of stimulation with BAY 41-2272. *B–D*: Effects of BAY 41-2272 (*B*), the cGMP analog 8-bromo-cGMP (*C*), and the protein kinase G inhibitor KT-5823 in the presence of BAY 41-2272 (*D*) on hypoxia-inducible factor (HIF)-1α protein expression induced by hypoxia in cultured cardiomyocytes. Shown are representative images of Western blots, and values are given as means ± SE for 4-samples. $^*P < 0.05$ and $^{**}P < 0.01$ vs. control/normoxia. $^{\#}P < 0.05$ and $^{\#\#}P < 0.01$ vs. hypoxia in the absence of any treatment. $^+P < 0.05$ vs. hypoxia in the presence of BAY 41-2272. β-Actin was used for protein loading.

Table 1. *Hemodynamics, heart and lung weight, and cGMP level*

	Sham	AC	AC + BAY 41-2272
Systolic blood pressure, mmHg	122±4	194±5*	183±3*
Diastolic blood pressure, mmHg	89±2	157±8*	155±8*
Heart rate, beats/min	340±42	408±58	378±7
Heart weight/body weight, mg/g	3.2±0.1	4.4±0.2*	4.3±0.2*
Lung weight/body weight, mg/g	4.2±0.1	4.8±0.8	4.0±0.2
cGMP in LV, fmol/mg protein	972±89	1,665±73	2,208±411†

Data are expressed as means ± SE; $n = 4$ for systolic/diastolic blood pressure and heart rate; $n = 6$ (sham), 10 [aortic constriction (AC)], and 10 (AC + BAY 41-2272) for the other parameters. LV, left ventricle. *$P < 0.01$ and †$P < 0.05$ vs. sham group.

Western blot. Equal amounts of denatured total protein (20 μg) or nuclear extract (10 μg) from the LV or cultured cardiomyocytes were subjected to SDS-polyacrylamide gel as described (36). In brief, the separated proteins electrically transferred onto polyvinylidene difluoride (PVDF) membranes were incubated with 5% skim milk. PVDF membranes were then incubated with a monoclonal antibody against HIF-1α (0.25 μg/ml, clone H1alpha67; Novus Biologicals) or VEGF (0.4 μg/ml, VG1; abcam) followed by a horseradish peroxidase-coupled secondary antibody. Immunoreactive bands were visualized with the ECL Plus detection kit (Amersham), and intensity of each band was analyzed densitometrically (Chemi Doc Documentation System; Bio-Rad).

Radioimmunoassay. cGMP level in the LV and in the cultured cells were determined using a radioimmunoassay kit (YAMASA Cyclic GMP Assay Kit) as previously described (22).

Statistical analysis. All data were analyzed with SPSS software version 11.0 (SPSS). Values are expressed as means ± SE. Differences between two groups were analyzed by Student's *t*-test, and differences between three groups were assessed using one-way ANOVA followed by Scheffé's test. Survival analysis was performed using the Kaplan-Meier method, and statistical significance was accepted at $P < 0.05$.

RESULTS

In vitro effects of BAY 41-2272 and cGMP pathway on hypoxic induction of HIF-1α expression in cultured cardiomyocytes. Figure 1*A* shows that BAY 41-2272 (5×10^{-5} mol/l) significantly ($P < 0.05$) increased the intracellular cGMP level in cultured cardiomyocytes. At this concentration, BAY 41-2272 had little effect on the protein expression of HIF-1α under normoxic conditions, but significantly ($P < 0.01$) inhibited the hypoxia-induced expression of HIF-1α (Fig. 1*B*). A cGMP analog, 8-bromo-cGMP (10^{-3} mol/l), decreased the expression of HIF-1α induced by hypoxia (Fig. 1*C*), whereas the inhibition of protein kinase G by KT-5823 (10^{-6} mol/l) reversed the inhibitory effect elicited by BAY 41-2272 (Fig. 1*D*).

In vivo effects of BAY 41-2272 on systemic blood pressure, heart and lung weight, and cGMP level. As shown in Table 1, the AC significantly ($P < 0.01$) increased the systolic and diastolic blood pressure levels compared with the sham group, whereas BAY 41-2272 had little effect on the elevation of blood pressure induced by pressure overload. In addition, the AC significantly ($P < 0.01$) increased the ratio of heart weight

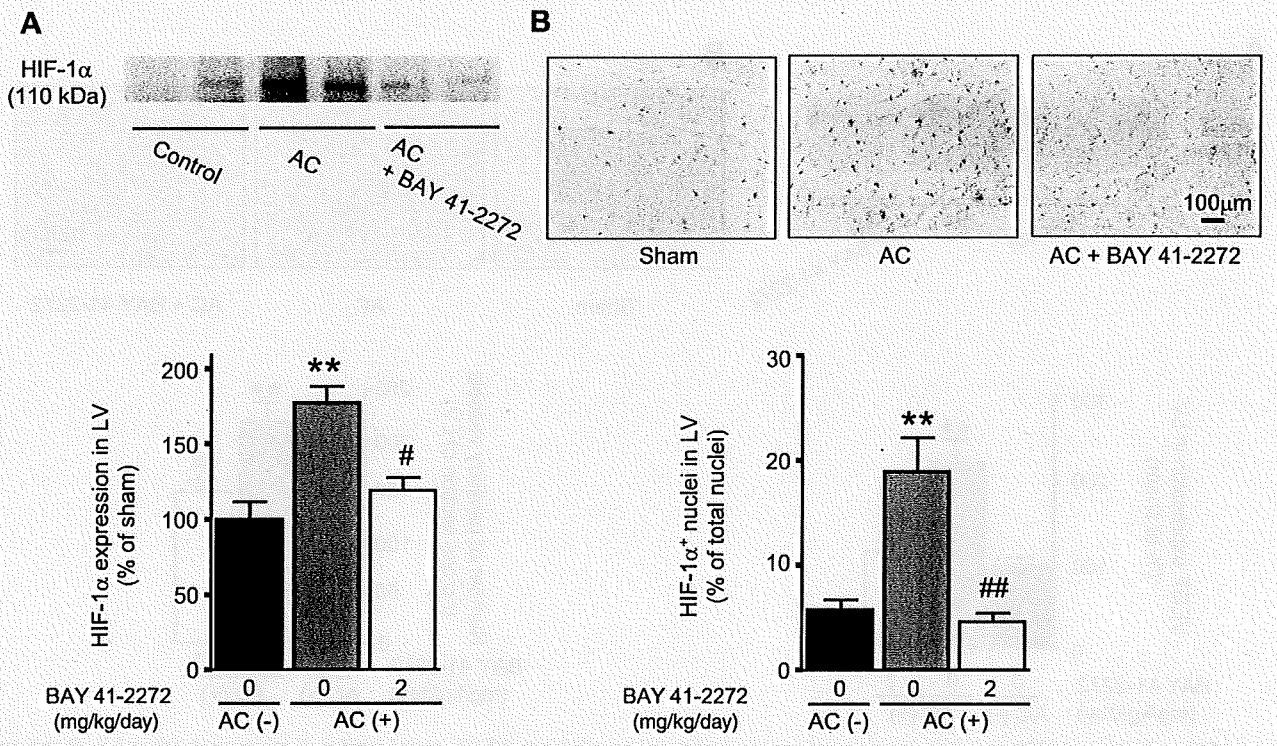

Fig. 2. Effects of BAY 41-2272 on protein expression of HIF-1α (*A*) and number of HIF-1α-positive nuclei (*B*) in the left ventricle (LV). Shown are representative images of Western blot (*A*) and distribution of immunoreactive HIF-1α (*B*) in the sham and aortic constriction (AC) without or with BAY 41-2272 treatment group. Values are shown as means ± SE for 6–10 samples. **$P < 0.01$ vs. the sham group. #$P < 0.05$ and ##$P < 0.01$ vs. the AC group without BAY 41-2272 treatment.

to body weight compared with the sham group. However, it was not affected by the BAY 41-2272 treatment. BAY 41-2272 treatment had a trend to further increase the cGMP level in the LV of AC rats. Neither the heart rate nor the ratio of lung weight to body weight was changed in the respective groups.

Effect of BAY 41-2272 on HIF-1α protein expression induced by pressure overload. Figure 2*A* shows that the protein level of HIF-1α in the LV was significantly ($P < 0.01$) increased by the AC but was significantly ($P < 0.05$) decreased by the BAY 41-2272 treatment. As shown in Fig. 2*B*, the number of nuclei positive for HIF-1α in the cardiocytes was significantly ($P < 0.01$) increased by the AC but was significantly ($P < 0.01$) reduced by the treatment.

Effects of BAY 41-2272 on VEGF protein expression and number of capillary vessels induced by pressure overload. Figure 3*A* shows that the protein level of VEGF in the LV was significantly ($P < 0.01$) increased by the AC but was significantly ($P < 0.01$) decreased by the BAY 41-2272 treatment. Figure 3*B* shows that the AC significantly ($P < 0.01$) increased the number of capillary vessels in the LV; however, BAY 41-2272 significantly ($P < 0.01$) decreased the number by 32%.

Effect of BAY 41-2272 on infiltration of monocyte/macrophages induced by pressure overload. Figure 4 shows that monocyte/macrophages significantly ($P < 0.05$) increased in number, accumulating around the intramyocardial arteries in the LV induced by pressure overload. BAY 41-2272 significantly ($P < 0.05$) decreased the number by 84%.

Survival rate. Figure 5 shows that BAY 41-2272 administration in the AC rats significantly ($P = 0.0395$) reduced the mortality over 14-day periods. Heart failure was the main cause of death, as confirmed by postmortem examination (pulmonary edema or hemorrhage was noted in most of the dead rats).

DISCUSSION

In this study, we report that pharmacological stimulation of sGC-cGMP decreased the hypoxia-induced HIF-1α expression in cultured cardiomyocytes. In addition, the subdepressor dose of BAY 41-2272 modulated the protein expressions of HIF-1α and VEGF and the number of capillary vessels induced by pressure overload.

The beneficial effects of stimulating sGC-cGMP on hemodynamics and remodeling in cardiovascular disorders have been demonstrated by ourselves and others (3, 6, 7, 18, 22, 23). The present study extends our understanding of the important biological action for sGC-cGMP stimulation on improving the survival following the AC. However, the mechanisms by which the stimulation of sGC would affect the remodeling process remain to be defined. In this study, we specifically focused on the interaction between HIF-1α and sGC-cGMP in cardiomyocytes exposed to hypoxia and in LV during mechanical load. As shown, BAY 41-2272 reduced the hypoxia-induced HIF-1α expression in cultured cardiomyocytes, and this was accompanied by an increase in the intracellular cGMP level. In addition, a cGMP analog mimicked the effect of BAY 41-2272 on HIF-1α expression, whereas the inhibition of protein kinase G reversed the effect of BAY 41-2272 on HIF-1α expression induced by hypoxia in these cells. These results suggest that the activation of sGC/cGMP/protein kinase

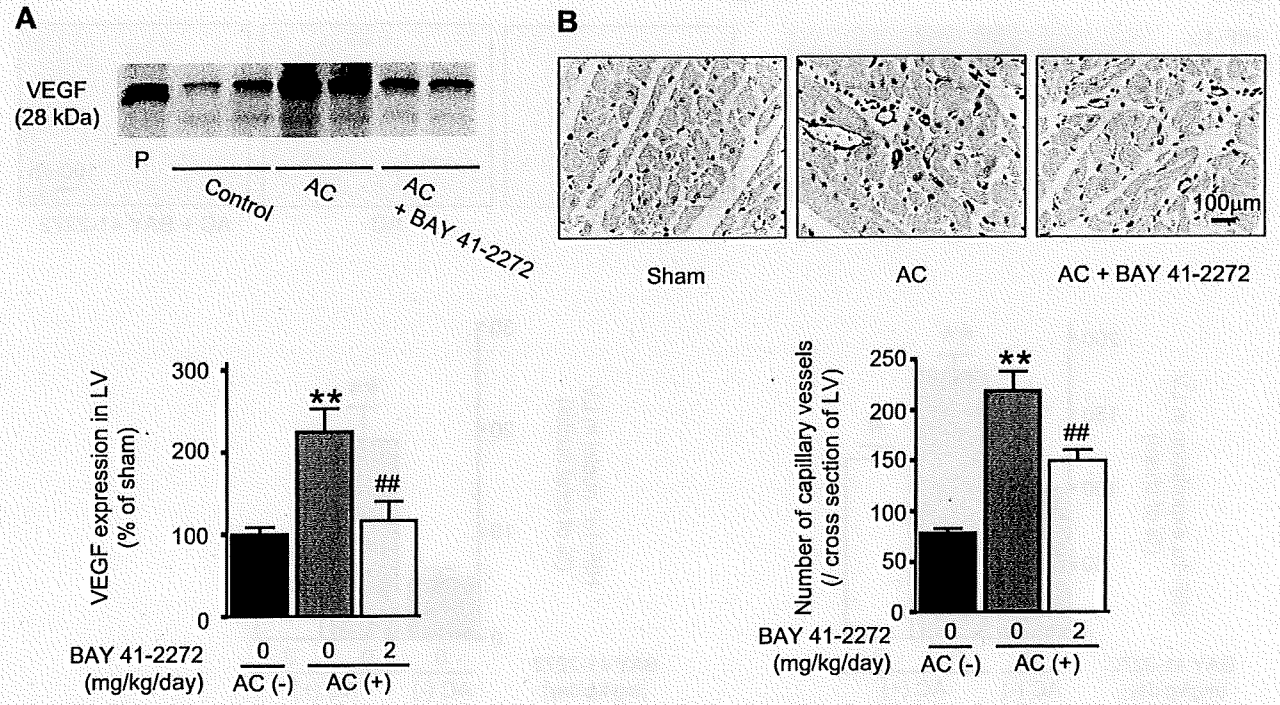

Fig. 3. Effects of BAY 41-2272 on protein expression of vascular endothelial growth factor (VEGF; *A*) and number of microvessels (*B*) in LV. Shown are representative images of Western blot for VEGF (*A*) and distribution of microvessels stained with von Willebrand factor (vWF) (*B*) in the sham and AC without or with BAY 41-2272 treatment group. Values are shown as means ± SE of 6–10 samples examined. $^{**}P < 0.01$ vs. the sham group. $^{\#\#}P < 0.01$ vs. the AC group without BAY 41-2272 treatment. P, positive control (rat kidney) for VEGF.

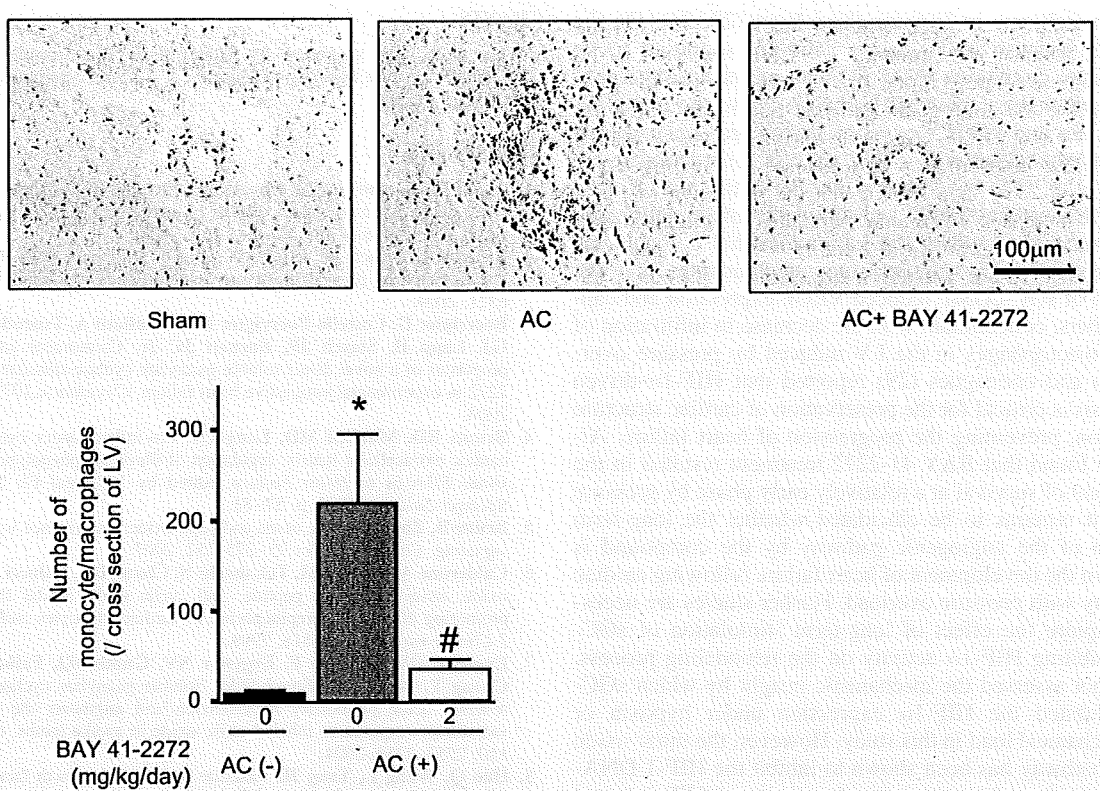

Fig. 4. Effect of BAY 41-2272 on number of monocyte/macrophages in the LV. Shown are representative images of distribution of monocyte/macrophages stained with CD68 antigen in the sham and AC without or with BAY 41-2272 treatment group. Values are shown as means ± SE for 6–10 samples examined. $P < 0.05$ vs. the sham group (*) and vs. the AC group without BAY 41-2272 treatment (#).

G signaling directly downregulates HIF-1α expression in cultured cardiomyocytes under hypoxic conditions. Mechanical load and/or tissue ischemia has been suggested to stimulate the HIF-1α expression during the pressure overload to the heart (17, 29). Our study supports that the HIF-1α expression was increased in the pressure-overloaded LV. On the other hand, the role of sGC-cGMP signaling in modulating HIF-1α and VEGF expressions is reported to be dependent on oxygen supply (1, 5, 20, 27). In the present study, BAY 41-2272 had little effect on the HIF-1α expression under normoxic conditions, but the compound significantly inhibited the expression under the hypoxia in cultured cardiomyocytes. Comparable with this, the protein expressions of HIF-1α and VEGF and the number of capillary vessels were attenuated by the compound in pressure-overloaded LV. As reported previously (30), the immunoreactivity to HIF-1α accumulated in nuclei in the cardiocytes of LV induced by pressure overload, but it was significantly decreased by the treatment, implying that the change in HIF-1α expression in cardiocytes altered the angiogenic activity in a paracrine fashion (29). Thus it seems that BAY 41-2272 counteracted the HIF-1α induction and angiogenic process during pressure overload. Mechanical load induces the multiple signal transductions, stimulating cardiomyocyte hypertrophy and fibrosis (28). Despite the almost complete inhibition of pressure overload-induced increase in HIF-1α by treatment with BAY 41-2272, the corresponding increase in capillary density was partially inhibited, suggesting that HIF-1α was not the only stimulus driving the increased capillary density. It might be explained that other pathways also coordinate to induce the angiogenic gene transcription independent of HIF-1α during the pressure overload (21, 40).

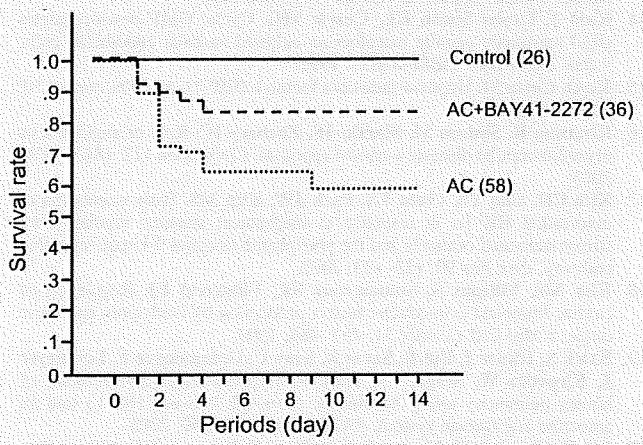

Fig. 5. Effect of BAY41-2272 on survival rate. Kaplan-Meier survival analysis showed a significant reduction of mortality by the BAY41-2272 treatment during the pressure overload (Log rank test; $P = 0.0395$). Parenthesis in the respective group indicates the number of rats.

It appears case-dependent whether angiogenesis is beneficial or detrimental in the progression of cardiovascular diseases (8, 12, 13, 16, 42). As capillary vessels supply oxygen and nutrients to the cardiocytes in response to the demand; angiogenesis would be beneficial for maintaining the structure and

function in ischemic or hypertrophied heart (29, 34). On the other hand, because inflammatory cells are supposed to be recruited from circulating blood (4), one might raise the concern of whether the angiogenic pathway due to the upregulation of HIF-1α and VEGF expression during pressure overload is related to the inflammation and adverse remodeling (8, 9, 31). Zhao et al. (42) have shown that the inhibition of nitric oxide/cGMP increases VEGF and stimulates inflammation and arteriosclerosis surrounding the intramyocardial coronary arteries. Conversely, the present study demonstrates that the stimulation of sGC-cGMP reduced VEGF expression and capillary numbers, concomitant with the decrease in infiltration of monocyte/macrophages in the LV induced by pressure overload. Sano and colleagues (29) reported that HIF-1α-driven angiogenesis is critical for the preservation of cardiac structure and function, preventing the progression of heart failure. Although we found that BAY 41-2272 treatment resulted in the improvement of survival at a relatively early phase by pressure overload, it remains to be elucidated whether the long-term attenuation of the angiogenic pathway by the compound is beneficial in the development of heart failure following cardiac hypertrophy with pressure overload. Further studies are necessary to explore the effect of long-term stimulation of sGC-cGMP inhibiting HIF-1α activity on the remodeling process. We have not assessed the mechanistic insight by which sGC-cGMP inhibited the HIF-1α expression under hypoxia or during mechanical load in this study. However, the nitric oxide signaling pathway has been shown to inhibit the HIF-1 DNA-binding activity and transcriptional activity of HIF-1 target genes in hypoxic cells (11, 20, 32). Therefore, we speculate that the sGC-cGMP stimulation with BAY 41-2272 might have a similar action of nitric oxide under those conditions. In addition, cGMP signaling has been shown to regulate a number of genes with regard to angiogenesis, inflammation, and extracellular matrix (25). Thus it remains unknown whether all of these effects that we observed in this study are explicably mediated by the change in HIF-1α. We have reported that the BAY 41-2272 treatment attenuated the fibrosis induced by pressure overload, accompanied by inhibiting the activity of angiotensin-converting enzyme and the subsequent decrease in the concentration of ANG II in the heart (23). HIF-1α drives not only angiogenesis but regulates the transcription of a number of genes for cell survival/proliferation, matrix metabolism, and vascular tone in a tissue-specific manner (15). Alternatively, the present study might support that the HIF-1α contributes to the syntheses of tissue angiotensin-converting enzyme (19) and extracellular matrix-related genes (9) directly during pressure overload, whereas the sGC-cGMP stimulation would have reversed the remodeling of heart at least in part by modulating the HIF-1α expression.

In summary, this study supports that the HIF-1α expression is upregulated under hypoxia in the cultured cardiomyocytes and in the cardiocytes of pressure-overloaded LV. In addition, our data imply a possible involvement of HIF-1α expression modulated by the pharmacological sGC-cGMP stimulation in regulating the LV remodeling.

ACKNOWLEDGMENTS

We thank Dr. Johannes-Peter Stasch (Bayer Schering Pharma) for providing BAY 41-2272 compound and stimulating discussion. We also thank Ritsuko Sotomura for technical assistance.

GRANTS

This work was supported by Grants-in-aid for Scientific Research (20590830) from the Ministry of Education, Culture, Sports, Science, and Technology, Japan.

REFERENCES

1. **Agani FH, Puchowicz M, Chavez JC, Pichiule P, LaManna J.** Role of nitric oxide in the regulation of HIF-1α expression during hypoxia. *Am J Physiol Cell Physiol* 283: C178–C186, 2002.
2. **Bischoff E, Stasch JP.** Effects of the sGC stimulator BAY 41-2272 are not mediated by phosphodiesterase 5 inhibition. *Circulation* 110: e320–e321, 2004.
3. **Boerrigter G, Costello-Boerrigter LC, Cataliotti A, Tsuruda T, Harty GJ, Lapp H, Stasch JP, Burnett JC Jr.** Cardiorenal and humoral properties of a novel direct soluble guanylate cyclase stimulator BAY41-2272 in experimental congestive heart failure. *Circulation* 107: 686–689, 2003.
4. **Brown RD, Mitchell MD, Long CS.** Pro-inflammatory cytokines and cardiac extracellular matrix: regulation of fibroblast phenotype. In: *Interstitial Fibrosis in Heart Failure*, edited by Villarreal FJ. New York: Springer Science, 2005, p. 57–81.
5. **Brüne B, Zhou J.** Nitric oxide and superoxide: interference with hypoxic signaling. *Cardiovasc Res* 75: 275–282, 2007.
6. **Calderone A, Thaik CM, Takahashi N, Chang DL, Colucci WS.** Nitric oxide, atrial natriuretic peptide, and cyclic GMP inhibit the growth-promoting effects of norepinephrine in cardiac myocytes and fibroblast. *J Clin Invest* 101: 812–818, 1998.
7. **Evgenov OV, Ichinose F, Evgenov NV, Gnoth MJ, Falkowski GE, Chang Y, Bloch KD, Zapol WM.** Soluble guanylate cyclase activator reverses acute pulmonary hypertension and augments the pulmonary vasodilator response to inhaled nitric oxide in awake lambs. *Circulation* 110: 2253–2259, 2004.
8. **Hao Q, Wang L, Tang H.** Vascular endothelial growth factor induces protein kinase D-dependent production of pro-inflammatory cytokines in endothelial cells. *Am J Physiol Cell Physiol* 296: C821–C827, 2009.
9. **Higgins DF, Biju MP, Akai Y, Wutz A, Johnson RS, Haase VH.** Hypoxic induction of Ctgf is directly mediated by Hif-1. *Am J Physiol Renal Physiol* 287: F1223–F1232, 2004.
10. **Hirano S, Imamura T, Onitsuka H, Matsuo T, Kitamura K, Koiwaya Y, Eto T.** Rapid increase in cardiac adrenomedullin gene expression caused by acute pressure overload: effect of the renin-angiotensin system on gene expression. *Circ J* 66: 397–402, 2002.
11. **Huang LE, Willmore WG, Gu J, Goldberg MA, Bunn HF.** Inhibition of hypoxia-inducible factor 1 activation by carbon monoxide and nitric oxide. Implications for oxygen sensing and signaling. *J Biol Chem* 274: 9038–9044, 1999.
12. **Isner JM.** Still more debate over VEGF. *Nat Med* 7: 639–641, 2001.
13. **Kai H, Kuwahara F, Tokuda K, Imaizumi T.** Diastolic dysfunction in hypertensive hearts: roles of perivascular inflammation and reactive myocardial fibrosis. *Hypertens Res* 28: 483–490, 2005.
14. **Kato J, Lanier-Smith KL, Currie MG.** Cyclic GMP down-regulates atrial natriuretic peptide receptors on cultured vascular endothelial cells. *J Biol Chem* 266: 14681–14685, 1991.
15. **Ke Q, Costa M.** Hypoxia-inducible factor-1 (HIF-1). *Mol Pharmacol* 70: 1469–1480, 2006.
16. **Khurana R, Simons M, Martin JF, Zachary IC.** Role of angiogenesis in cardiovascular disease: a critical appraisal. *Circulation* 112: 1813–1824, 2005.
17. **Kim CH, Cho YS, Chun YS, Park JW, Kim MS.** Early expression of myocardial HIF-1α in response to mechanical stresses: regulation by stretch-activated channels and the phosphatidylinositol 3-kinase signaling pathway. *Circ Res* 90: e25–e33, 2002.
18. **Kim NN, Villegas S, Summerour SR, Villarreal FJ.** Regulation of cardiac fibroblast extracellular matrix production by bradykinin and nitric oxide. *J Mol Cell Cardiol* 31: 457–466, 1999.
19. **Krick S, Hänze J, Eul B, Savai R, Seay U, Grimminger F, Lohmeyer J, Klepetko W, Seeger W, Rose F.** Hypoxia-driven proliferation of human pulmonary artery fibroblasts: cross-talk between HIF-1α and an autocrine angiotensin system. *FASEB J* 19: 857–859, 2005.
20. **Liu Y, Christou H, Morita T, Laughner E, Semenza GL, Kourembanas S.** Carbon monoxide and nitric oxide suppress the hypoxic induction of vascular endothelial growth factor gene via the 5′ enhancer. *J Biol Chem* 273: 15257–15262, 1998.

21. **Mammoto A, Connor KM, Mammoto T, Yung CW, Huh D, Aderman CM, Mostoslavsky G, Smith LE, Ingber DE.** A mechanosensitive transcriptional mechanism that controls angiogenesis. *Nature* 457: 1103–1108, 2009.
22. **Masuyama H, Tsuruda T, Kato J, Imamura T, Asada Y, Stasch JP, Kitamura K, Eto T.** Soluble guanylate cyclase stimulation on cardiovascular remodeling in angiotensin II-induced hypertensive rats. *Hypertension* 48: 972–978, 2006.
23. **Masuyama H, Tsuruda T, Sekita Y, Hatakeyama K, Imamura T, Kato J, Asada Y, Stasch JP, Kitamura K.** Pressure-independent effects of pharmacological stimulation of soluble guanylate cyclase on fibrosis in pressure overloaded rat heart. *Hypertens Res* 32: 597–603, 2009.
24. **Opie LH, Commerford PJ, Gersh BJ, Pfeffer MA.** Controversies in ventricular remodelling. *Lancet* 367: 356–367, 2006.
25. **Pilz RB, Broderick KE.** Role of cyclic GMP in gene regulation. *Front Biosci* 10: 1239–1268, 2005.
26. **Pugh CW, Ratcliffe PJ.** Regulation of angiogenesis by hypoxia: role of the HIF system. *Nat Med* 9: 677–684, 2003.
27. **Pyriochou A, Beis D, Koika V, Potytarchou C, Papadimitriou E, Zhou Z, Papapetropoulos A.** Soluble guanylyl cyclase activation promotes angiogenesis. *J Pharmacol Exp Ther* 319: 663–671, 2006.
28. **Ruwhof C, van der Laarse A.** Mechanical stress-induced cardiac hypertrophy: mechanisms and signal transduction pathways. *Cardiovasc Res* 47: 23–37, 2000.
29. **Sano M, Minamino T, Toko H, Miyauchi H, Orimo M, Qin Y, Akazawa H, Tateno K, Kayama Y, Harada M, Shimizu I, Asahara T, Hamada H, Tomita S, Molkentin JD, Zou Y, Komuro I.** p53-induced inhibition of Hif-1 causes cardiac dysfunction during pressure overload. *Nature* 446: 444–448, 2007.
30. **Shyu KG, Liou JY, Wang BW, Fang WJ, Chang H.** Carvedilol prevents cardiac hypertrophy and overexpression of hypoxia-inducible factor-1α and vascular endothelial growth factor in pressure-overloaded rat heart. *J Biomed Sci* 12: 409–420, 2005.
31. **Sluimer JC, Gasc JM, van Wanroij JL, Kisters N, Groeneweg M, Sollewijn Gelpke MD, Cleutjens JP, van den Akker LH, Corvol P, Wouters BG, Daemen MJ, Bijnens AP.** Hypoxia, hypoxia-inducible transcription factor, and macrophages in human atherosclerotic plaques are correlated with intraplaque angiogenesis. *J Am Coll Cardiol* 51: 1258–1265, 2008.
32. **Sogawa K, Numayama-Tsuruta K, Ema M, Abe M, Abe H, Fujii-Kuriyama Y.** Inhibition of hypoxia-inducible factor 1 activity by nitric oxide donors in hypoxia. *Proc Natl Acad Sci USA* 95: 7368–7373, 1998.
33. **Stasch JP, Becker EM, Alonso-Alija C, Apeler H, Denbowsky K, Feurer A, Gerzer R, Minuth T, Perzborn E, UP, Schröder H, Schroeder W, Stahl E, Steinke W, Straub A, Schramm M.** NO-independent regulatory site on soluble guanylate cyclase. *Nature* 410: 212–215, 2001.
34. **Tomanek RJ.** Response of the coronary vasculature to myocardial hypertrophy. *J Am Coll Cardiol* 15: 528–533, 1990.
35. **Tsuruda T, Boerrigter G, Huntley BK, Noser JA, Cataliotti A, Costello-Boerrigter LC, Chen HH, Burnett JC Jr.** Brain natriuretic peptide is produced in cardiac fibroblasts and induces matrix metalloproteinases. *Circ Res* 91: 1127–1134, 2002.
36. **Tsuruda T, Kato J, Hatakeyama K, Kojima K, Yano M, Yano Y, Nakamura K, Nakamura-Uchiyama F, Matsushima Y, Imamura T, Onitsuka T, Asada Y, Nawa Y, Eto T, Kitamura K.** Adventitial mast cells contribute to pathogenesis in the progression of abdominal aortic aneurysm. *Circ Res* 102: 1368–1377, 2008.
37. **Tsuruda T, Kato J, Hatakeyama K, Masuyama H, Cao YN, Imamura T, Kitamura K, Asada Y, Eto T.** Antifibrotic effect of adrenomedullin on coronary adventitia in angiotensin II-induced hypertensive rats. *Cardiovasc Res* 65: 921–929, 2005.
38. **Tsuruda T, Kato J, Kitamura K, Kuwasako K, Imamura T, Koiwaya Y, Tsuji T, Kangawa K, Eto T.** Adrenomedullin: a possible autocrine or paracrine inhibitor of hypertrophy of cardiomyocytes. *Hypertension* 31: 505–510, 1998.
39. **Wen JF, Cui X, Jin JY, Kim SM, Kim SZ, Kim SH, Lee HS, Cho KW.** High and low gain switches for regulation of cAMP efflux concentration: distinct roles for particulate GC- and soluble GC-cGMP-PDE3 signaling in rabbit atria. *Circ Res* 94: 936–943, 2004.
40. **Yang R, Amir J, Liu H, Chaqour B.** Mechanical strain activates a program of genes functionally involved in paracrine signaling of angiogenesis. *Physiol Genomics* 36: 1–14, 2008.
41. **Zhang Q, Molino B, Yan L, Haim T, Vaks Y, Scholz PM, Weiss HR.** Nitric oxide and cGMP protein kinase activity in aged ventricular myocytes. *Am J Physiol Heart Circ Physiol* 281: H2304–H2309, 2001.
42. **Zhao Q, Egashira K, Inoue S, Usui M, Kitamoto S, Ni W, Ishibashi M, Hiasa K, Ichiki T, Shibuya M, Takeshita A.** Vascular endothelial growth factor is necessary in the development of arteriosclerosis by recruiting/activating monocytes in a rat model of long-term inhibition of nitric oxide synthesis. *Circulation* 105: 1110–1115, 2002.

アドレノメデュリンの発見

Discovery of adrenomedullin

北村和雄

Key words：アドレノメデュリン，PAMP，褐色細胞腫，cAMP，アドレノメデュリン前駆体

1. アドレノメデュリン発見の背景

心房性ナトリウム利尿ペプチドやエンドセリンなどの発見により新しい循環調節機構が明らかになってきたように，複雑で精巧な循環調節機構を解明していくためには，まだ同定されていない新しい循環調節因子を単離し，構造的に明らかにすることが新たな研究の展開のために重要である．宮崎医科大学(現宮崎大学医学部)の松尾・寒川グループからは，50種類近くの新規生理活性ペプチドの発見とそれに続く基礎的・臨床的研究を展開してきており，我が国が世界に誇りうる業績を残している(**図1**)．このような生理活性ペプチドの探索研究の基礎となったのが，1970年代に行われていたオピオイド研究である．脳内に存在する微量の生理活性ペプチドを単離・構造決定するために，それまでの方法論が見直され，改良された．

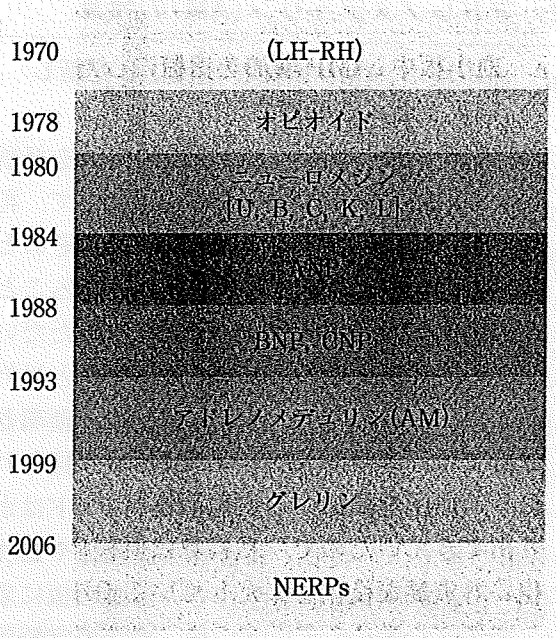

図1　生理活性ペプチドの発見(松尾・寒川グループの貢献)

松尾・寒川グループからは，50種類近くの新規生理活性ペプチドの発見とそれに続く基礎的・臨床的研究を展開してきている．なお，NERPsは松尾・寒川グループ出身の南野らのグループで発見された．

生化学的にモノを扱う研究でまず重要なことは，生体内からモノを抽出する際に，生体内で存在する分子型のままで取り出し，安定化させることである．このために，組織をH_2O中で煮沸後に抽出するという方法が確立された．この方法により内在性のペプチドを生体内で存在する分子型のまま安定化させるとともに，タンパクがプロテアーゼにより分解されて生じるペプチドを最小限に抑えることができ，目的の生理活性ペプチドの精製が容易になった．更に，その当時出てきた高速液体クロマトグラフィや気相式シークエンサーにより，高感度化が進み，比較的少量の組織から生理活性ペプチド探索研究ができるようになった．また，生理活性ペプチドの活性を測定する方法も開発され，摘出平滑筋を用いた非特異的なバイオアッセイにより，

Kazuo Kitamura: Department of Internal Medicine, Circulatory and Body Fluid Regulation, Faculty of Medicine, University of Miyazaki　宮崎大学医学部 内科学講座 循環体液制御学分野

0047-1852/09/¥40/頁/JCOPY

多くのニューロメジン類が発見された．このように生理活性ペプチド探索研究の方法論が確立されるときに，私は大学院生として在籍しており，今考えると，得難い経験と勉強ができたと感じている．そして，大学院4年のときに，私の直接指導をしてくれていた寒川先生が心房性ナトリウム利尿ペプチドを数カ月で単離・構造決定し，グローバルに活躍されるようになるのを見て，私も将来は自分自身の生理活性ペプチドを発見して，研究を展開したいと思うようになった．

2. アドレノメデュリン(AM)の発見

a. 血小板中cAMP増加を指標にした新しいアッセイ法の確立[1]

大学院終了後しばらく大学病院の医員を経験した後，米国に留学し，1988年に帰国して，再び第1内科で仕事をするようになった．そのとき，私自身が教室や大学のために役立てることは，松尾先生・寒川先生より指導していただいたペプチド探索研究の方法論を生かすこと以外にはないと考えていた．当時は高血圧・循環器の分野では，エンドセリンやBNPが発見されており，血圧を調節する生理活性ペプチドはかなり出てきていたので，私自身は血栓症や動脈硬化にも重要な役割を果たしている血小板に着目して研究を進めることにした．当時の宮崎医科大学の内科学第一講座では，アンジオテンシン変換酵素阻害薬の血小板機能に及ぼす影響についての研究がされていたこともあり，血小板凝集機能の検査の機器がそろっていたことも，血小板に作用するペプチドの探索を考えた理由の一つである．

最初のうちはウサギやヒトの血小板に対する凝集能で生理活性ペプチドの探索を試みたが，再現性や感度の面でうまくいかなかった．それで，血小板中cAMP上昇が血小板機能を抑制することをヒントにして，ラット血小板の浮遊液(50μL)にペプチド検体(50μL)を加え37°Cで反応させた後，産生されたcAMPをラジオイムノアッセイ(RIA)で測定し，その増加を活性の指標とする方法を作成した．本アッセイ法は簡便で，高感度ではあったが，未知の生理活性ペプチドの探索法とするためには，再現性に問題があった．

再現性の悪い理由の一つとして，アッセイごとに調製する血小板のばらつきが考えられ，最初にそれについて検討したが改良はみられなかった．当初著者らは，反応時間を長くするとcAMP産生量も増加するので，アッセイの精度も上がるものと考え，5分あるいは10分間の反応時間で行っていた．しかし，5分と10分での結果を比較すると，反応時間の短い5分の方で，血小板中cAMP濃度がコントロールと比較して高く，更にばらつきが少ない傾向が認められたため，次に反応時間について細かく検討を行った．その結果，30秒と極端に短時間の反応を行うことにより，高感度で再現性の高い結果が得られることが明らかになった．血小板中では検体刺激によりcAMPはごく短時間で上昇するが，その後反応性にphosphodiesteraseが活性化し，血小板中cAMPが減少してしまうためだと考えている．

このようにして我々は，簡便かつ高感度で再現性の高いアッセイ法という，未知物質検索のための新たな方法論を手にすることができた．研究を開始して，新たなアッセイ系を確立するために，既に2年近くの歳月を要していた．

b. 血小板中cAMP増加活性を指標にしたペプチドの系統的検索[2]

苦労して確立した上記のアッセイ法を用いて，未知のペプチドの検索を開始した．しかし，新しいアッセイ法が確立できたからといって，簡単に新規ペプチドが発見できたわけではなかった．我々はそれまでの微量生理活性ペプチドの検索には，大量の組織の入手が容易であるブタの組織を出発材料として用いており，新しいアッセイ法による検索においてもブタの脳，消化管，心臓などの抽出物を用いて検討していたが，それらの組織からは新規ペプチドへの手がかりは得られていなかった．

当時の宮崎医科大学第1内科では，褐色細胞腫の患者は1年に1症例あるかないかであった．全くの偶然だと思われるが，血小板中cAMP増